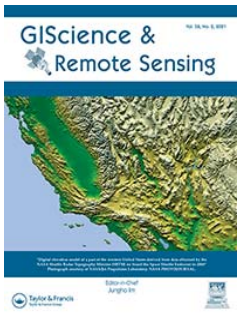

GIScience & Remote Sensing

ISSN: (Print) (Online) Journal homepage: https://www.tandfonline.com/loi/tgrs20

# Quantitatively distinguishing the impact of climate change and human activities on vegetation in mainland China with the improved residual method

Yahai Zhang & Aizhong Ye

**To cite this article:** Yahai Zhang & Aizhong Ye (2021) Quantitatively distinguishing the impact of climate change and human activities on vegetation in mainland China with the improved residual method, GIScience & Remote Sensing, 58:2, 235-260, DOI: 10.1080/15481603.2021.1872244

**To link to this article:** https://doi.org/10.1080/15481603.2021.1872244

Published online: 12 Jan 2021.

GISCIENCE & REMOTE SENSING
2021, VOL. 58, NO. 2, 235–260
https://doi.org/10.1080/15481603.2021.1872244



# Quantitatively distinguishing the impact of climate change and human activities on vegetation in mainland China with the improved residual method

Yahai Zhang and Aizhong Ye

State Key Laboratory of Earth Surface Processes and Resource Ecology, Faculty of Geographical Science, Beijing Normal University, Beijing, China

**ABSTRACT**

In recent decades, vegetation has faced the dual challenges posed by climate change and human activities. Quantitatively distinguishing the influences of climate change and human activities on vegetation changes is key to developing adaptive ecological protection policies. This study examined changes in temperature and precipitation to determine if anthropogenic land use changes have affected vegetation in mainland China. The contribution rates of temperature and precipitation changes and land use changes to vegetation dynamics are further calculated by the improved residual trend method, which considers the nonlinear relationship between vegetation and climate factors and time-lag effects from a spatiotemporal perspective and sets the base period for the equation. The results show that 68.81% of the vegetation in mainland China is in a state of sustained growth, where cultivated vegetation and grasses are the main greening vegetation types. The contribution of land use changes to vegetation changes in mainland China is higher than that of temperature and precipitation changes. Planting trees and grasses and returning farmlands to forests and grassland has increased the area covered by grasses and mixed coniferous broad-leaved forests, while cultivated vegetation coverage has decreased. Swamps are more sensitive to temperature and precipitation changes. We show that the improved residual trend method that considers temporal and spatial dimensions can reduce the uncertainty in quantifying the effects of climatic and anthropogenic factors on vegetation dynamics. This study provides a theoretical basis and a useful tool for future governmental implementation of ecological management strategies.

**ARTICLE HISTORY**
Received 11 June 2020
Accepted 3 January 2021

**KEYWORDS**
NDVI; climate change; human activities; mainland China; residual trend

## 1. Introduction

Vegetation plays a vital role in ecosystems and is an indicator of the health and stability of an ecological environment (Bégué et al. 2011; de Jong et al. 2011; Foley et al. 2000). The normalized vegetation index (NDVI) is the difference between the reflectance received in the near-infrared band and that in the red band divided by their sum (Tucker, Holben, and Goff 1984). It can accurately reflect the surface vegetation coverage and is widely used in the detection of regional or global vegetation growth (Xu, Wang, and Yang 2017; Faour, Mhawej, and Nasrallah 2018; Lamchin et al. 2018). NDVI has limitations and can be easily saturated in areas with high vegetation cover (Gu et al. 2013). Although the enhanced vegetation index (EVI) is superior to the NDVI in characterizing areas with high vegetation coverage, the calculation of EVI is limited only to sensor systems with blue bands, so it is difficult to obtain long time series such as NDVI and is susceptible to the influence of topography (Huete, Justice, and Van Leeuwen 1999; Son et al. 2014; Testa et al. 2018). NDVI has the advantages of having a high sensitivity and spatial and temporal adaptability for detecting vegetation, making it the most commonly implemented vegetation index in large-scale and long-term detection studies (Bai, Yang, and Jiang 2019; Fensholt and Proud 2012). According to a report by the Intergovernmental Panel on Climate Change (IPCC), the main driving force of current climate change is the increase in anthropogenic $CO_2$ emissions (Cui et al. 2020). The main features of climate change include climate warming and an increase in the occurrence of extreme events. The growth of vegetation is mainly affected by temperature and precipitation (Fatima et al. 2020). Vegetation has been significantly affected by global climate change in recent years (Pettorelli et al. 2005; Chen, Hu, and Yu 2005; Guo et al. 2014; Nemani et al. 2003; Bao et al. 2014). Studies have

**CONTACT** Aizhong Ye azye@bnu.edu.cn

shown that global warming has caused significant changes in vegetation coverage across the Northern Hemisphere, especially at high latitudes (Beck et al. 2011; Slayback et al. 2003; Menzel et al. 2006). In addition, the impact of human activities on vegetation cannot be ignored, such as that of urbanization, population migration, land use change, vegetation construction and soil and water conservation engineering, etc (Neigh, Tucker, and Townshend 2008; Wu et al. 2013; Hua and Chen 2013). For example, overexploitation and overgrazing have led to the degradation of grasslands in Central Asia and Mongolia. (Jiang et al. 2017; Hilker et al. 2014). The Chinese government launched the Grain to Green Program (GTGP), which has been demonstrated to have improved vegetation coverage on the Loess Plateau (Zhou, Zhao, and Zhu 2012; Sun et al., 2015b). These human activities are mainly expressed as land use changes. In this study, we focus on the increasing coverage of urban land, reduction of cultivated land, and changes in the abundance of grasslands and forests.

Over the past 30 years, the vegetation coverage in China as a whole has shown a tendency to increase, but there is an obvious interannual pattern, with a rapid increase before the 1990s, followed by a slow growth period and then a rapid recovery during the 21st century (Liu et al. 2015; Peng et al. 2011; Piao et al. 2015). However, vegetation is affected by both climate- and human-related activities and behaves differently in different areas. For example, in the more economically developed Yangtze River Delta and Pearl River Delta, the vegetation coverage has decreased (Du et al. 2019), while in the Loess Plateau region, the vegetation coverage has increased significantly due to the return of croplands to forests and grasslands (Li, Peng, and Li 2017; Xie et al. 2015). China is one of the countries in the world that has been severely affected by climate change due to its diverse and changing climatic conditions (Liu and Raven 2010; Ren et al. 2005). Studies have shown that the rate of increase in China's average annual temperature over the past few decades is significantly higher than the global average over the same period (Shi et al. 2018; Ying 2012). In addition, regional differences in precipitation trends in China are obvious; droughts are worsening in the north, while the frequency and intensity of flood events are increasing in the south (Xu et al. 2011; Zhou, Ding, and Wang 2010; Gong, Pan, and Wang 2004; Zhai and Panmao 2003; Qian and Lin 2005; Zhai et al. 2005). Conversely, significant changes have taken place in the regional land use patterns in mainland China, and various land use types have undergone transformations. Since 1998, the Chinese government has successively implemented six major forestry projects, the return of farmland to forest and grass, soil and water conservation and other measures (Xu et al. 2018b). Vegetation has undergone dramatic changes due to the coupling of climate change and human activities (Zhang et al. 2016; Sun et al., 2015a; Wang et al. 2015; Zhang et al. 2016). However, the response of vegetation to climate change remains uncertain, and the impact of human activities on vegetation is twofold. Most studies now focus on the combined effects of climate- and anthropogenic-impacts on NDVI, and it is difficult to distinguish or even quantify the respective effects of these two factors on vegetation (Xie et al. 2015; Hua et al. 2017). It is, therefore, necessary to isolate the effects of climate change and human activities on the observed vegetation changes.

Quantitative research on the contribution of climate change and human activities to vegetation changes is mainly focused on areas with a fragile ecosystem in China, such as the Chinese Loess Plateau (Zheng et al., 2019b), inner Mongolian (Mu et al. 2013), Tibetan Plateau (Pan et al. 2017) and three-river source region (Zhang et al. 2016). There is an overall lack of quantitative assessment of all of mainland China. Although studies have detected the trend of greening in China, quantified the contribution of carbon dioxide concentration rise and nitrogen deposition and pointed out that human activities may play a role in promoting vegetation change (Piao et al. 2015), there has been no quantitative contribution to the distinction between the effects of human activities and climatic changes on vegetation change. Currently, there are three main types of methods used to quantitatively distinguish between the effects of climate change and human activity on changes in vegetation cover: regression model methods, residual trend methods and NPP-based biophysical modeling methods. The residual trend method is the most widely used method to separate and quantitatively analyze climate changes and human activities (Evans and Geerken 2004; Higginbottom and Symeonakis 2014). Each of these three methods used for quantifying the relative contributions of climate change and

human activities to vegetation change has advantages and disadvantages. Regression analysis is easy to preform, and the required data are easy to obtain; however, it treats vegetation change as a simple linear relationship between the influencing factors and does not take into account the autocorrelation between the respective variables (Liu et al. 2015; Li et al. 2016;). The NPP-based model is the most complex of the three methods and can accurately reflect the driving factors behind vegetation changes. However, this method is subject to a high degree of uncertainty, including the fact that across different models, different driver data and different study scales can lead to large variability in the results (Chen et al. 2014; Xu, Wang, and Yang 2017; Zhang et al. 2019). The residual trend method is simple and effective, and it reflects the spatial drivers well. It can be used to quantify the contribution rate through the application of a regression equation between the NDVI and climate factors (Tong et al. 2017; Li, Peng, and Li 2017). It is difficult, however, to define periods without anthropogenic impacts, and the categories of anthropogenic activities and active periods vary considerably by region. Conversely, the relationship between the climate factors and NDVI is not simple and linear, and there are time lag effects, so there are errors resulting from the use of linear regression equations. Due to the limitations of the original residual trend method (Burrell, Evans, and Liu 2017), before application to different regions, it must be adjusted and improved to better identify the impacts of climate changes and human activities on changes in vegetation (Li, Peng, and Li 2017; Zhang and Shunfeng 2003).

This study attempts to improve the residual trend method to analyze the temporal and spatial vegetation dynamics of mainland China from 1982 to 2015 to quantify its response to climate change and human activities. Climate change in this study refers to changes in temperature and precipitation. In addition, human activities in this article refer to anthropogenic land use changes, which directly affect changes in vegetation cover. The shortcomings of the residual trend method are threefold: (1) The prediction equation is built without considering the effects of human activities in the year in which it is built, which can lead to bias in the prediction equation itself. (2) The nonlinear response to NDVI to the climate factors are not considered when constructing the prediction equation between the NDVI values and the climate factors. (3) The time lag effect of climate change on vegetation growth is not considered. Current research suggests that vegetation changes may be influenced not only by current climatic conditions but also by preclimatic factors (Kong et al. 2020; Wu et al. 2015; Zhao et al. 2020), making it necessary to consider the effects of time lags when studying the relationship between climate factors and vegetation. To improve the assessment capabilities of the residual trend method, we use NDVI mutation points to set up time nodes to establish the relationship between climate factors and NDVI values, i.e., the assumption that the effects of human activities on vegetation change can be ignored during the period before the mutation point. Second, nonlinear multiple regression equations are established to find the lag of NDVI on climate factors using deterministic coefficients. Finally, spatial prediction equations are built for different vegetation types to mitigate the uncertainty associated with the residual trend method. The objectives of this paper are as follows: (1) improve the residual trend method to make it more reasonable and applicable and (2) quantitatively distinguish the contribution rate of climate change (represented by temperature and precipitation) and human activities (represented by the area of land use change caused by ecological engineering and urbanization) to vegetation changes in mainland China. Due to the influences of human activities, regional land use in mainland China is undergoing changes, with transformations occurring between land use types, such as farmland changing to forests and grasslands. We mainly calculated the conversion area of farmland, constructed land and unused land from 1982 to 2015 to verify the impact of human activities on vegetation change. We hope to gain an understanding of the status of the vegetation in mainland China affected by the dual effects of climate change and human activities, which will assist in the establishment of scientific ecological protection measures to achieve sustainable development.

## 2. Study site & data

### *2.1. Study site*

Mainland China is located in East Asia, which is largely defined as China's territory, excluding most of China's

coastal islands (including Taiwan Island, South China Sea Islands and Diaoyu Island). China has a vast territory, a wide latitude, varied distances from the sea and various terrain types; thus, the combination of temperature and precipitation is diverse, forming a variety of climate types. Most of the types of vegetation in the world can be found in China due to the complex and diverse climate. In this research, mainland China is divided into 17 basins (Figure 1) to represent relatively different climatic characteristics among these basins (Lang et al. 2014), which has been widely used across many studies (e.g., Ma, Yuan, and Ye 2015; Ma et al. 2016, 2018; Zhang and Ye 2020). The label of every basin seen in Figure 1 corresponds to Table 1.

## 2.2. Data

### 2.2.1. NDVI data

The Global Inventory Monitoring and Modeling Studies (GIMMS3g v1) NDVI dataset (Pinzon and Tucker 2014) is synthesized every half month from 1982 to 2015 at a spatial resolution of 0.083°, released by the National Aeronautics and Space Administration (NASA) and obtained by the Advanced Very High-resolution Radiometer (AVHRR) sensors on the National Oceanic and Atmospheric Administration (NOAA) satellite. The GIMMS3g NDVI dataset is processed using adaptive empirical pattern decomposition (EMD) to remove artifacts from the sequence, including differences in the data due to differences between sensors, making it a more stable dataset (Ibrahim et al. 2015). The maximum value composite (MVC) method was adopted for calculating the monthly data to remove noise (Holben and Brent 2007). In addition, areas with NDVI values less than 0.1 are set to 0.1 to shield areas not covered by vegetation. Statistical analysis of the average NDVI value for each basin was performed. The GIMMS3g NDVI dataset has the highest temporal consistency compared to other NDVI products and is the most suitable choice for NDVI trend analysis (Fensholt and Proud 2012; Ibrahim et al. 2015; Zhou, Yamaguchi, and Arjasakusuma 2018). The GIMMS3g NDVI dataset is used extensively in terrestrial vegetation research (de Jong et al. 2011; Mao et al. 2012; Peng et al. 2011; Wang and Han 2012; Wu et al. 2016).

### 2.2.2. Climate data

The growth of vegetation is generally mainly affected by three climate factors, precipitation (52% of the climatic controls), temperature (31%) and radiation (5%); radiation mainly influences tropical rainforests (Churkina and Running 1998; Bonan 2008; Nemani et al. 2003; Schuur 2003). China's tropical rainforests are small and sparsely distributed

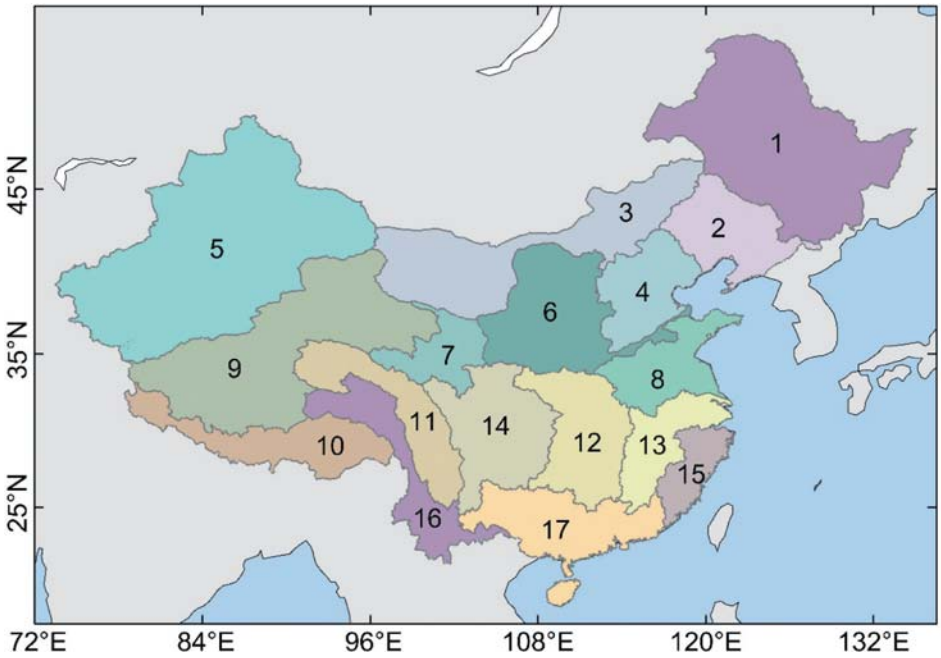


**Figure 1.** The 17 basins in Mainland China.

**Table 1.** The information of the 17 basins in China (Lang et al. 2014; Peel, Finlayson, and McMahon 2007).

| Region | Full name | Mean Annual prec. (mm) | Mean Annual temp. (°C) | Main Land use types (in descending order) | Area (km2) |
|---|---|---|---|---|---|
| 1 | Songhua River | 535.5 | 1.1 | Forest, Farmland, Grassland | 370,973 |
| 2 | Liao River | 566.1 | 6.1 | Farmland, Forest, Grassland | 310,117 |
| 3 | Inner Mongolia inland river | 220.4 | 5.1 | Unused land, Grassland, Farmland | 1,537,520 |
| 4 | Hai River | 515.9 | 8.8 | Farmland, Forest, Grassland | 578,092 |
| 5 | Inland rivers in Xinjiang | 168.3 | 5.9 | Unused land, Grassland, Farmland | 1,104,104 |
| 6 | Lower Yellow River | 391.0 | 8.5 | Grassland, Farmland, Forest | 448,864 |
| 7 | Upper Yellow River | 469.3 | −0.7 | Grassland, Forest, Unused land | 504,731 |
| 8 | Huai River | 819.5 | 14.4 | Farmland, Constructed land, Forest | 415,287 |
| 9 | Inland rivers in Northern Tibet | 199.9 | −1.8 | Grassland, Unused land, Water | 694,413 |
| 10 | Brahmaputra | 876.7 | 0.5 | Grassland, Forest, Unused land | 908,881 |
| 11 | Upper Yangtze River | 795.2 | 0.6 | Grassland, Forest, Unused land | 399,541 |
| 12 | Middle and Lower Yangtze River | 1276.5 | 14.7 | Forest, Farmland, Grassland | 567,237 |
| 13 | Lower Yangtze River | 1606.5 | 16.7 | Forest, Farmland, Water | 324,061 |
| 14 | Middle and Upper Yangtze River | 1001.1 | 11.0 | Forest, Farmland, Grassland | 323,970 |
| 15 | Southeastern River | 1705.9 | 16.6 | Forest, Farmland, Grassland | 226,496 |
| 16 | Lancang River | 882.2 | 7.3 | Grassland, Forest, Unused land | 316,057 |
| 17 | Pearl River | 1700.7 | 19.0 | Forest, Farmland, Grassland | 567,520 |

and are mainly found in the southern Taiwan Province and Hainan Province and the estuary and Xishuangbanna regions in southern Yunnan (Zheng et al. 2019a; Zhu 2013). Therefore, we did not consider the radiation factor. In this study, the parameters of precipitation and temperature were selected for research. China's Ground Precipitation 0.5° × 0.5° Grid Data Set version 2.0 and China's Ground Temperature 0.5° × 0.5° Grid Data Set version 2.0 produced by the National Meteorological Information Center of China were used to calculate the monthly total precipitation and the monthly average temperature. The thin plate spline (TPS) interpolation method of ANUSPLIN was adopted to generate gridded precipitation and temperature data based on daily meteorological materials from 2472 national meteorological observation stations distributed over mainland China. To further determine the relationship between the NDVI and climate factors, we resampled the 1982–2015 precipitation and temperature grid data to 0.083°× 0.083°, which is the same resolution as the GIMMS3g NDVI dataset. Additionally, the monthly and annual average temperature and total precipitation of the basin were calculated.

### 2.2.3. Vegetation-type data

The vegetation-type data are provided by the Data Center for Resources and Environmental Sciences, Chinese Academy of Sciences (RESDC) (http://www.resdc.cn). The spatial distribution of the vegetation types was obtained from the 1:1000000-China digital vegetation map (Hou 2001). The data are mainly based on the results of vegetation investigations and research carried out in all parts of the country over the past 50 years. Eleven types of vegetation were recognized, including cultivated vegetation (CV), alpine plant (AP), swamp, meadow, grass, grassland, desert, shrubland, broad-leaved forest (BF), mixed coniferous and broad-leaved forest (MCBF), coniferous forest (CF) and others (Figure 2). In this paper, the names of the 12 vegetation types match those in Figure 2.

Since most of the NDVI values for the other and desert classifications were below 0.1, we screened out NDVI values less than 0.1; these areas were not included in our study. Therefore, we only studied the remaining 10 types of quilts.

### 2.2.4. Land use data

This study uses remote sensing monitoring data of land use status in China for 1980, 2000 and 2015. The dataset was downloaded from the Data Center for Resources and Environmental Sciences, Chinese Academy of Sciences (RESDC) (http://www.resdc.cn). The land use types of the dataset include six primary

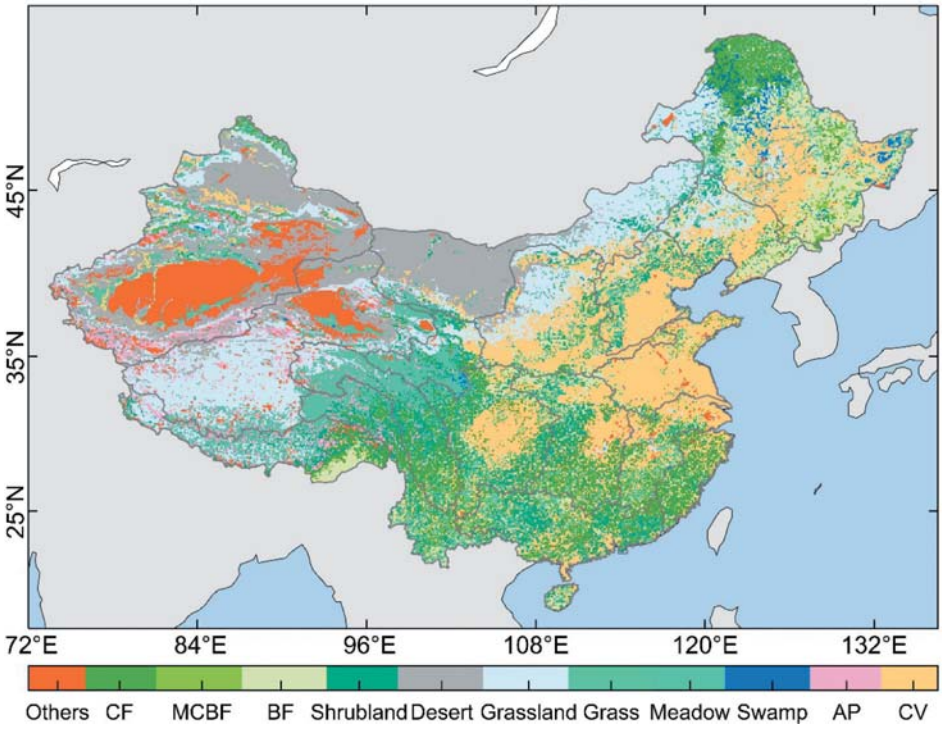


**Figure 2.** The vegetation distribution map of mainland China at a scale of 1:1000000.

types: farmland, forest, grassland, water, constructed land and unused land.

## 3. Methods

### 3.1. Change analysis methods

In this study, the slope of the linear regression is used to express the rate of interannual change of each factor, and the slope is optimized by using the least squares method to minimize the sum of its squared errors (Cai and Hall 2006; Ramsay 1977). When the slope>0, the elemental sequence increased across the time steps; conversely, when the slope<0, the elemental sequence decreased, and the larger the absolute value of the slope was, the greater the rate of change of the element.

The slope of the fitting function can be expressed as follows:

$$Slope = \frac{n\sum_{i=1}^{n} i \times x_i - \sum_{i=1}^{n} i \sum_{i=1}^{n} x_i}{n\sum_{i=1}^{n} i^2 - \left(\sum_{i=1}^{n} i\right)^2} \quad (1)$$

where Slope is the trend in the factor time series, n is the number of monitoring years, which varied from 1 to 34, and $x_i$ represents the element value corresponding to the *i*-th year.

The coefficient of variation (*cv*) is the ratio of the standard deviation of a set of data to the average value. *cv*is a statistic that measures the degree of fluctuation in a data set, which can eliminate the influences of measurement scale and dimension. The *cv* can be expressed as follows:

$$cv = \frac{\sigma}{\mu} \quad (2)$$

$$\sigma = \sqrt{\frac{1}{n \cdot 1}\sum_{i=1}^{n} (x_i - \bar{x})^2} \quad (3)$$

where *cv* is the coefficient of variation, $\sigma$and$\mu$are the standard deviation and the mean value of a group of data, respectively, *n* is the number of data points, *i*=1, 2, 3, … n, $x_i$ represents the *i*-th data point, and $\bar{x}$ represents the average of the data.

### 3.2. Pettitt test

To select a period with a presumed absence of human activity, the Pettitt test was used. The average of the

mutation years in each basin was taken as the mutation point for vegetation cover change.

The Pettitt test (Pettitt 1979) is a non-parametric test used for detecting a single inflection point in a time series. In the present study, the Pettitt test was applied to obtain a significant inflection point in the annual value of NDVI. This method uses the Mann-Whitney statistic $U_{t,N}$ to test whether the samples $x_1$, $x_2$, $x_3$, …, $x_t$ and $x_{t+1}$, $x_{t+2}$, $x_{t+3}$, …, $x_N$ have the same distribution. The $U_{t,N}$ time series is obtained using the following equation:

$$U_{t,N} = U_{t-1,N} + \sum_{j=1}^{N} \mathrm{sgn}(x_i - x_j) \tag{4}$$

where t = 2 …, N. If $\theta$>0, then sgn ($\theta$) = 1; if$\theta$=0, then sgn ($\theta$) = 0; and if$\theta$<0, the sgn ($\theta$) = −1. The $k_N$ and *p*statistic is obtained using the following equation:

$$k_N = \mathrm{Max}_{1\le t\le N}|U_{t,N}| \tag{5}$$

$$p \cong 2\exp\left\{-6(k_n)^2/\left(N^3+N^2\right)\right\} \tag{6}$$

In this test, $H_0$ indicates smooth data, and $H_1$ indicates that a mutation occurred in the time series studied. If the calculated p-value is less than a significance level of 0.05, the point of change is considered statistically significant. In other words, $H_0$ has been rejected, and the change point is considered significant.

### 3.3. Improved RESTREND

The RESTREND (residual trend) method is used to distinguish the contribution rate of climate change and human activities to changes in vegetation cover by using the difference between the simulated vegetation change trend without human activities and the actual trends (Evans and Geerken 2004). Based on the RESTREND results (Burrell, Evans, and Liu 2017; Li et al. 2016; Liu et al. 2019; Xu et al. 2018b), we made some improvements to suit the circumstances in mainland China in the temporal and spatial dimensions.

In this study, the period of establishing the regression model is defined by the abrupt years of each basin. It is assumed that the growth of vegetation is not greatly disturbed by human activities before the inflection point of NDVI occurs in each basin, and this point is set as the base period (Figure 4). The residual value after the abrupt year in each basin is calculated. In addition, the NDVI values do not show simple linear relationship to precipitation and temperature (Kawabata, Ichii, and Yamaguchi 2001; Schultz and Halpert 1993; Wang, Rich, and Price 2003), and vegetation in mainland China has a time-lag effect on precipitation and temperature (Wu et al. 2015; Xu et al. 2014). This study establishes a binary nonlinear regression equation for which NDVI is the independent variable and precipitation and temperature are the dependent variables. In addition, the time-lag response from NDVI to climate factors was considered. The first step in calculation step is to establish a binary nonlinear equation that calculates various parameters, then the determined equation is used to calculate the predicted value of NDVI, and finally, the calculated difference between the observed value and predicted value of NDVI is obtained from remote sensing images. The specific formula is as follows:

$$NDVI_{pre} = a \times \ln P_{(i,n)} + b \times T_{(i,m)} + c \tag{7}$$

$$NDVI_{res} = NDVI_{obs} - NDVI_{pre} \tag{8}$$

where $NDVI_{pre}$ represents the predicted value of NDVI, $P_{(i,n)}$ represents the cumulative monthly precipitation (mm), $T_{(i,m)}$ represents the monthly average temperature(°C), *a*, *b*, and *c*represent the parameters of the regression model, *i* is the number of months, *n* and *m* represent the lag period of 0–3 months,$NDVI_{obs}$represents the observed NDVI values (GIMMS3g NDVI), and $NDVI_{res}$is the residual values of NDVI.

To determine the lagged month of precipitation and temperature and the best simulation equations, the determination coefficient $R^2$ was used to evaluate the goodness-of-fit of the regression model. $R^2$ is calculated as follows:

$$R^2 = 1 - \frac{\sum_{i=1}^{n}(x_i - \hat{x}_i)^2}{\sum_{i=1}^{n}(x_i - \bar{x})^2} \tag{9}$$

where $x_i$ is the true value of an element in the *i*-th month, $\hat{x}_i$ is the estimated value of the *i*-th month, $\bar{x}$ is the mean of the true value, and n is the number of samples. The closer the value of $R^2$is to 1, the better the fit of the developed equation is.

In terms of establishing regression equations, historical time series were used in the temporal dimension, while in the spatial dimension, we simulated the optimal hydrothermal conditions of different vegetation types.

The contribution of vegetation change can be attributed to the effects of climate change and human activities:

$$Climate = \frac{Slope(NDVI_{pre})}{|Slope(NDVI_{pre})| + |Slope(NDVI_{obs})|} \times 100\% \quad (10)$$

$$Human = \frac{Slope(NDVI_{res})}{|Slope(NDVI_{res})| + |Slope(NDVI_{obs})|} \times 100\% \quad (11)$$

where $Slope(NDVI_{pre})$, $Slope(NDVI_{obs})$, and $Slope(NDVI_{res})$ represent the trends of the annually predicted NDVI values, annually observed NDVI values and annual residual values, respectively. *Climate*(%) represents the contribution of climate change, and*Human* (%) represents the contribution of human activities. A positive (or negative) contribution ratio indicates a positive (or negative) influence on vegetation. A contribution ratio close to zero (i.e., between – 0.5% and +0.5%) indicates an insignificant effect on vegetation.

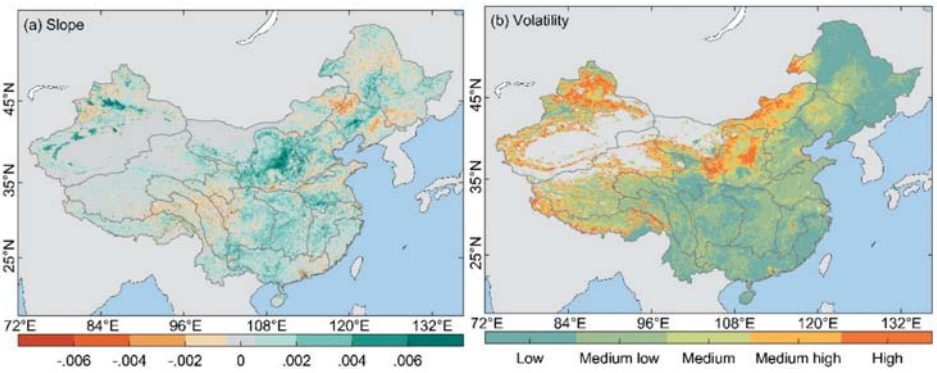


**Figure 3.** Changes in NDVI for mainland China from 1982 to 2015. (a) The slope of regression line; (b) Coefficient of variation (*cv*) of volatility.

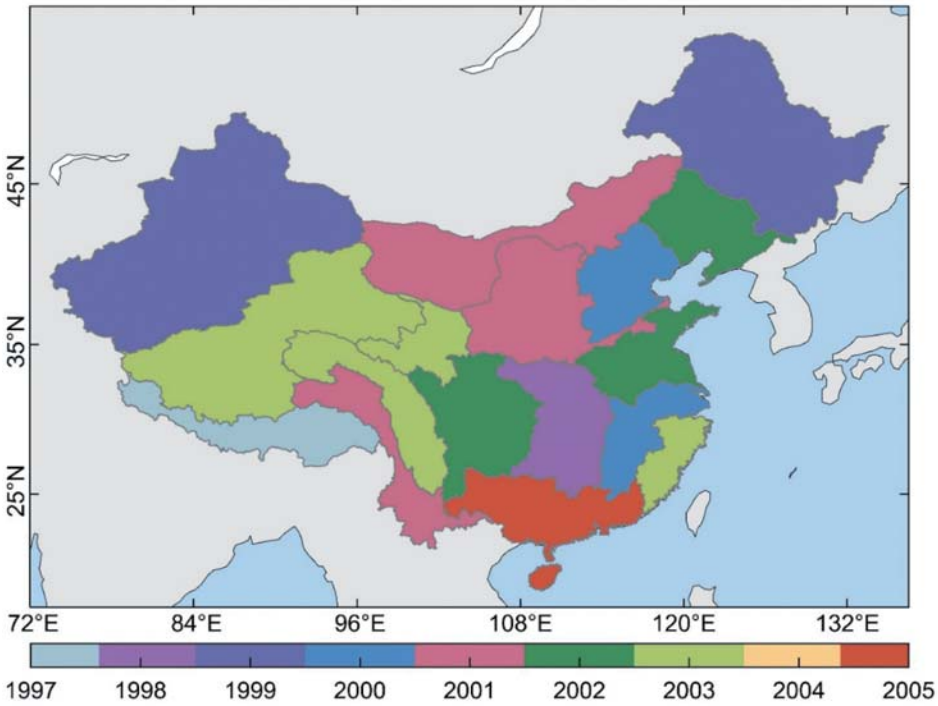


**Figure 4.** The inflection point of each basin in mainland China.

## 4. Results & discussion

### 4.1. The characteristics of vegetation change

The area of increase in vegetation coverage in mainland China accounted for 68.49%, with annual change rates centrally varying between −0.006/a and 0.006/a (Figure 3a). The regions with negative trends were mainly distributed over the northeast and the source regions of the Yangtze River, Yellow River and Lancang River. From 1982 to 2015, the coefficient of variation on NDVI in mainland China (Figure 3b) was 82.77% between 0.04 and 0.12, indicating that most of the vegetation changes in the study area were stable. Of the total area, 17.23% showed spatial differences, and the vegetation changes showed great volatility. Improvements in vegetation coverage were observed on the Loess Plateau, North China Plain and most of South Mainland China. In general, vegetation coverage changes in mainland China had spatially differentiated characteristics. The vegetation is expected to show a sustainable greening trend for the whole study area in the future.

Figure 4 shows the inflection point (the first significant year, $p < 0.05$) analysis results of the annual NDVI in the 17 basins from 1982 to 2015. The average years showing an abrupt change in each basin were between 1997 and 2005, which are concentrated around 2000. The Songhua River, Brahmaputra and Lancang River showed a decline in the NDVI after the inflection point, while the upward trend of NDVI of Inland rivers in Xinjiang, Hai River, Huai River and Upper Yangtze River slowed after the year of abrupt change. The NDVI of the remaining basins increased more significantly after the inflection year. Human activity in China in approximately 2000 and the timing of human activity vary across the regions (Piao et al. 2015). In the late 1990s, with the massive expansion of Chinese cities and the reduction in arable land (Tian, Zhuang, and Liu 2003; Deng et al. 2015; Jiyuan, Qian, and Yunfeng 2012), the vegetation coverage in Chinese cities declined (Sun 2012). Conversely, since 1999, the Chinese government has implemented a series of policies, such as tree planting and grass planting projects, that have greatly increased greening in China (Liu et al. 2018; Liu, Liu, and Li 2018; Chen et al. 2019).

It is assumed that in each basin within the time period preceding its inflection year, the vegetation change is less disturbed by anthropogenic land use changes. This allowed us to identify the effects of anthropogenic land use changes in the period following the previous baseline period.

### 4.2. The relationships between the NDVI and climate factors

#### 4.2.1. The lag-time effect between the NDVI and climatic factors

The lagged month of the response of vegetation in mainland to precipitation and temperature had obvious spatial variability. The time-lag effect of NDVI on precipitation was obtained, affecting 41.13% of the area in mainland China (Figure 5a). The areas with 3 lagged months for precipitation are mainly distributed in the southern part of the Brahmaputra, Lancang River and Upper Yangtze

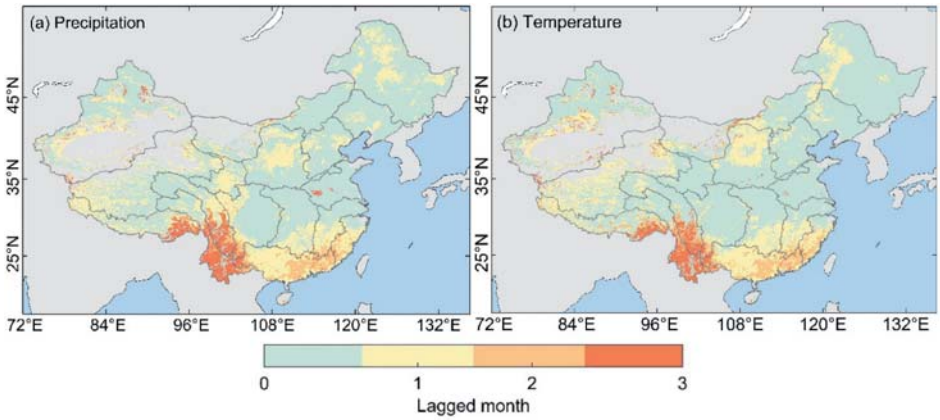


**Figure 5.** The lagged month at which the maximum determination coefficient of the regression equation between the NDVI and the total precipitation (mm) and average temperature (°C) is reported. (a) The lag time of NDVI response to precipitation. (b) The lag time of NDVI response to temperature.

River. A lagging period of 1–2 months can be found in the southern part of the Middle and Lower Yangtze River and Lower Yangtze River, as well as in the Pearl River and Southeastern River. In the response of NDVI in mainland China to precipitation, a 1-month lag can be found in the area accounted for 26.40%, and 2-month and 3-month lags affecting 7.20% and 7.53% of the area, respectively. In areas with sufficient precipitation, vegetation has sufficient water for photosynthesis, so the time lag effect on vegetation is more significant. The NDVI response to temperature in 60.73% of the area of mainland China has no time-lag effect (Figure 5b). The lag effect occurs mainly in southern mainland China, especially in the southern part of the Brahmaputra, Lancang River and Upper Yangtze River, with a lag time of 3 months. Areas with a 1-month lag, 2-month lag, and 3-month lag account for 23.28%, 8.08% and 7.91%, respectively.

The different vegetation types present in mainland China have significantly different time-lag effects on the response of NDVI to precipitation and temperature, and the same vegetation type also demonstrates different lagged months resulting from the combination of precipitation and temperature (Table 2). The lag effect of BF on precipitation is more obvious than that of temperature, with 73.10% of the area lagging behind 1–3 months. The 3-month precipitation time lag is mainly due to the two vegetation types, CF and MCBF, which account for 10.4% of the total coverage. Conversely, only 31.8% of the grasslands showed a time lag effect with precipitation, and a lag of 1-month accounts for 27.8%. The more temperature-sensitive vegetation types include BF, meadow, swamp and AP, which account for 73.1%, 72.9%, 73.6% and 69.6% of the area, respectively, all of which have a lag of 1–3 months.

#### 4.2.2. The spatial functional relationship between the NDVI and climate factors

To explore the possibility of establishing a regression equation in the spatial dimension, we further searched for the best hydrothermal conditions for the growth of each vegetation type. Although theoretical refinements have been made by assuming that the effect of human activity on vegetation changes prior to the year of the inflection is negligible, it is still not the optimal way to address the bias present in the prediction equation caused by the effects of human activities. Each vegetation type has its own adapted thermal and hydrothermal conditions under which it will grow naturally without interference from human activities. However, the equilibrium between the temperature and precipitation change and vegetation growth may be disrupted if disturbed by ecological engineering and urbanization. We build prediction equations from the spatial dimension and expect it to compensate for the temporal bias associated with anthropogenic effects. We presume that the growth of vegetation is affected less by human activities under the best hydrothermal conditions. Optimal thermal and hydrothermal conditions for each vegetation type were determined by fitting the multiyear monthly average precipitation and air temperature data to the NDVI. On the fitted curves, the optimum

**Table 2.** Statistics on the combination of precipitation and temperature time lag for various vegetation types in mainland China. P: precipitation; T: temperature.

| Lag time (month) | | The percentage of combined precipitation and temperature time lag for each vegetation type (%) | | | | | | | | | |
|---|---|---|---|---|---|---|---|---|---|---|---|
| P | T | CF | MC BF | BF | Shrub-land | Grass-land | Grass | Meadow | Swamp | AP | CV |
| 0 | 0 | 37.7 | 37.6 | 67.8 | 43.5 | 52.0 | 50.9 | 62.4 | 62.7 | 58.0 | 69.8 |
| 0 | 1 | 5.4 | 5.4 | 4.5 | 3.2 | 15.5 | 14.7 | 9.7 | 10.2 | 10.0 | 3.0 |
| 0 | 2 | 0.1 | 0.1 | 0.1 | 0.2 | 0.7 | 0.5 | 0.4 | 0.4 | 0.4 | 0.0 |
| 0 | 3 | 1.2 | 1.1 | 0.7 | 0.6 | 0.5 | 0.5 | 0.4 | 0.3 | 1.1 | 0.2 |
| 1 | 0 | 9.6 | 9.9 | 7.6 | 12.3 | 6.7 | 6.2 | 13.6 | 14.7 | 14.1 | 7.9 |
| 1 | 1 | 19.7 | 19.6 | 7.9 | 17.9 | 18.3 | 17.2 | 8.9 | 7.6 | 8.8 | 12.8 |
| 1 | 2 | 1.7 | 1.6 | 0.5 | 1.5 | 2.1 | 1.6 | 1.1 | 0.9 | 1.1 | 0.5 |
| 1 | 3 | 0.0 | 0.0 | 0.1 | 0.1 | 0.7 | 0.4 | 0.4 | 0.3 | 0.6 | 0.0 |
| 2 | 0 | 0.7 | 0.7 | 0.2 | 0.9 | 0.3 | 0.2 | 0.4 | 0.4 | 0.5 | 0.1 |
| 2 | 1 | 1.7 | 1.7 | 0.6 | 1.9 | 0.3 | 0.5 | 0.3 | 0.2 | 0.6 | 0.4 |
| 2 | 2 | 11.6 | 11.6 | 3.1 | 8.2 | 0.7 | 2.5 | 0.6 | 0.6 | 1.0 | 2.1 |
| 2 | 3 | 0.3 | 0.3 | 0.2 | 0.5 | 0.5 | 0.4 | 0.3 | 0.3 | 0.4 | 0.2 |
| 3 | 0 | 0.6 | 0.6 | 0.5 | 0.8 | 0.4 | 0.6 | 0.3 | 0.2 | 0.4 | 0.6 |
| 3 | 1 | 0.2 | 0.2 | 0.1 | 0.4 | 0.3 | 0.2 | 0.2 | 0.2 | 0.3 | 0.0 |
| 3 | 2 | 2.8 | 2.8 | 0.9 | 1.9 | 0.2 | 0.4 | 0.4 | 0.3 | 0.6 | 0.2 |
| 3 | 3 | 6.9 | 6.8 | 5.2 | 6.2 | 0.9 | 3.1 | 0.7 | 0.6 | 2.0 | 2.3 |

thermal and hydric conditions were determined as the interval where the NDVI values were

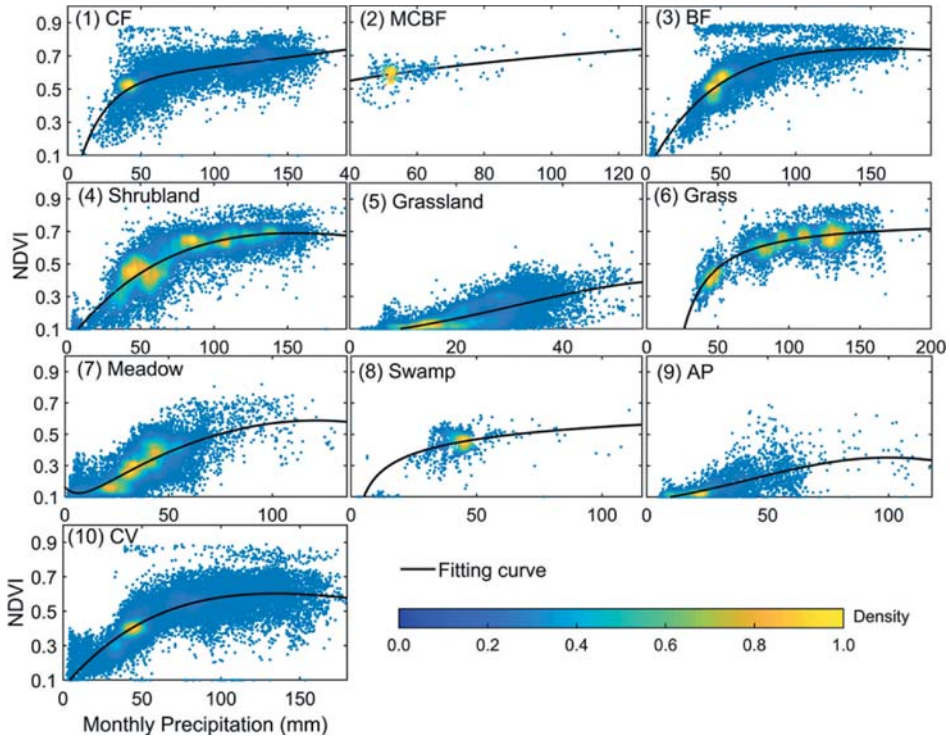


**Figure 6.** Scatter density plots and the curve fitted for the samples between NDVI and precipitation of the 10 vegetation types calculated by average monthly data during 1982–2015.

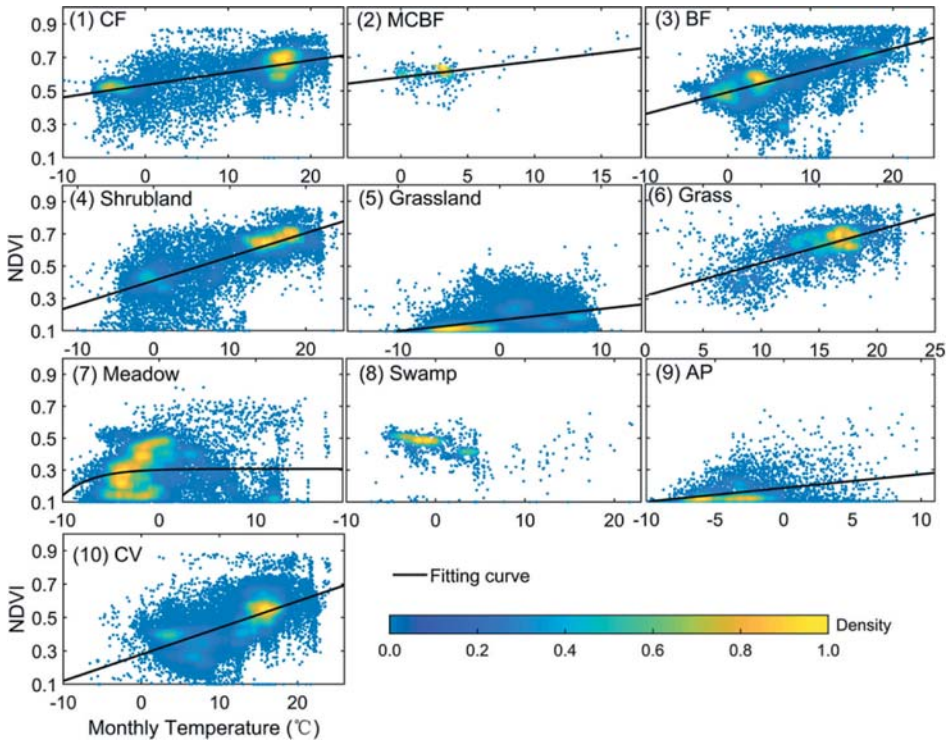


**Figure 7.** Scatter density plots and curve fitting for the samples between NDVI and temperature of the 10 vegetation types calculated using the average monthly data during 1982–2015.

approximately linearly related to precipitation and air temperature. According to scatter density plots, the fitted curves mostly occur in the high-density areas, indicating a good nonlinear relationship between precipitation and NDVI and a good linear relationship between temperature and NDVI. The functional relationship between NDVI and precipitation in mainland China is logarithmic, excluding that of MCBF, which is not as obvious (Figure 6). Vegetation growth increases with increasing precipitation, but when precipitation reaches a certain threshold, the rate of increase in NDVI obviously slows or even stops. The relationship between vegetation and temperature is linear, excluding that of shrubland and meadow (Figure 7). Within a certain interval, the NDVI value increase as temperature rises. Based on Figures 6 and 7, the optimal hydrothermal conditions were determined for each vegetation type (Table 3). The optimal precipitation range selected is the part where the rate of change of the fitted curve is largest. We deducted the range in which the NDVI does not respond drastically to changes in precipitation. Similarly, for temperature, we selected a temperature range with a higher point density near the fitted curve.

**Table 3.** The best hydrothermal conditions of different vegetation types in mainland China. P: Precipitation (mm/month).

| Vegetation type | Precipitation (mm/month) | Temperature (°C) |
|---|---|---|
| Others | 10–150 | −4-18 |
| CF | 9–70, if P > 70, NDVI = 0.7; if P < 9, NDVI = 0.15 | −6-22 |
| MCBF | 30–90, if P > 90, NDVI = 0.7; if P < 30, NDVI = 0.3 | −1-17 |
| BF | 10–105, if P > 105, NDVI = 0.8; if P < 10, NDVI = 0.1 | −5-24 |
| Shrubland | 15–100, if P > 100, NDVI = 0.75; if P < 15, NDVI = 0.1 | −4–22 |
| Desert | - | - |
| Grassland | 10–58 | −10-10 |
| Grass | 30–160, if P > 160, NDVI = 0.75; if P < 30, NDVI = 0.2 | 4-22 |
| Meadow | 15–80, if P > 80, NDVI = 0.7; if P < 15, NDVI = 0.1 | −8-13 |
| Swamp | 8–70, if P > 70, NDVI = 0.6; if P < 15, NDVI = 0.1 | - |
| AP | 11–111 | −10-10 |
| CV | 5–120, if P > 120, NDVI = 0.7; if P < 5, NDVI = 0.1 | 0–24 |

### 4.3. Model calibration

We used the predicted NDVI values calculated by the prediction model established in the base period of each basin to analyze the correlation with the observed NDVI values to verify the results of our improved method. The predicted NDVI values obtained by our improved method and the observed values show a higher correlation than that of the original method (Figure 8). Except in the inland rivers of Xinjiang (0.0645 lower than the original method) and inland rivers of northern Tibet (0.0461 lower than the original method), the correlation coefficient of the spatial dimension improvement method is lower than

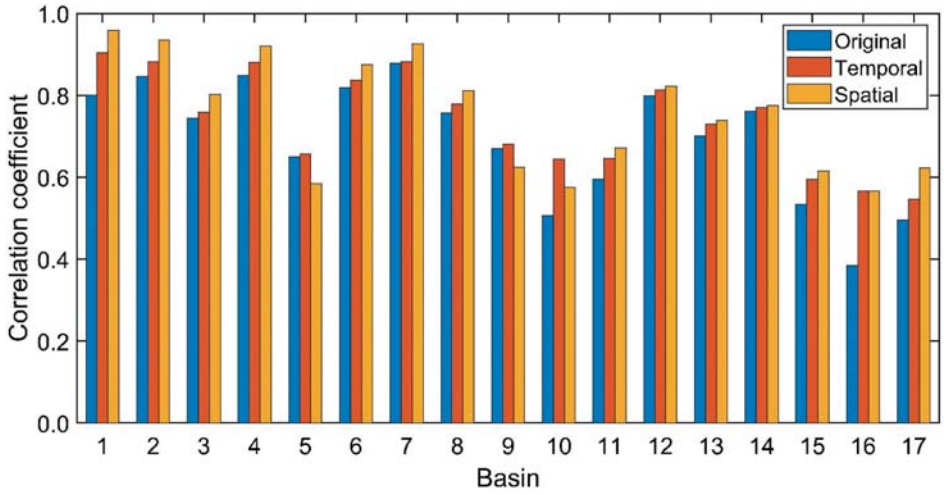


**Figure 8.** The correlation coefficient between the predicted NDVI values and the observed NDVI values averaged in each basin. The calculation period is from 1982 to before the inflection year of each basin.

that of the original method. This may be because, overall, the NDVI values of these two basins are relatively small. The correlation coefficients of the improved method in other basins are 0.0094 ~ 0.1815 higher than those of the original method and 0.0533 higher on average. The most obvious improvement was seen in the Songhua River (temporal dimension: 0.1815 higher; spatial dimension: 0.1807 higher) and the Southeastern River (temporal dimension: 0.1036 higher, spatial dimension: 0.1580 higher), and the correlation coefficients improved by more than 0.1. Overall, our improved method effectively modified the original method.

### 4.4. The contribution of climate change and human activities to NDVI change

From Figure 9, the positive and negative contributions of the temperature and precipitation changes and the anthropogenic land use changes to the temporal and spatial dimensions are similar overall in terms of their distribution characteristics, while there are some differences in a few regions, mainly

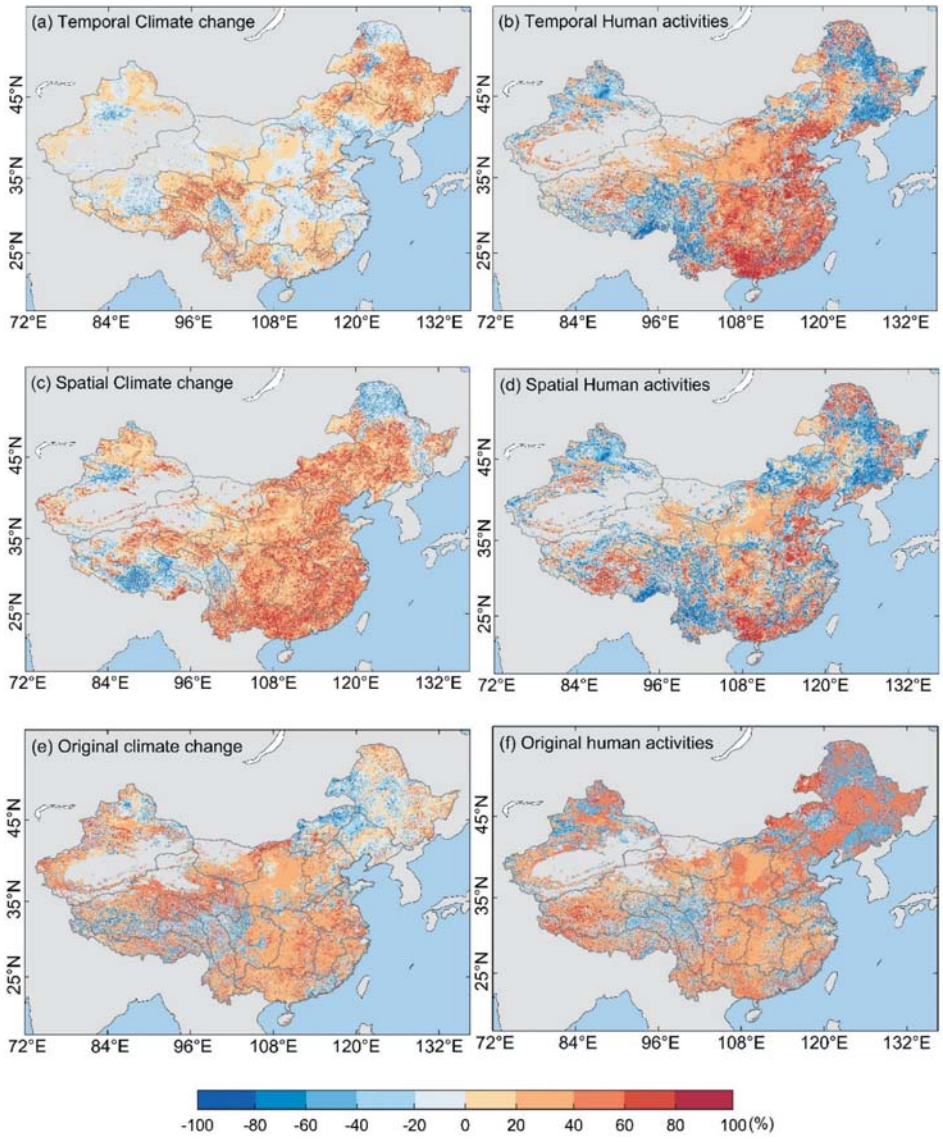


**Figure 9.** The contributions of climate change and human activities to NDVI in mainland China during 1982–2015. (a) The temporal contribution of climate change. (b) The temporal contribution of human activities. (c) The spatial contribution of climate change. (d) The spatial contribution of human activities. (e) The original contribution of climate change. (f) The original contribution of human activities.

in the Lower Yangtze River and the Brahmaputra. Areas with temperature and precipitation change contributions greater than 0 account for 58.47% of the temporal dimension (Figure 9a) and 78.91% of the spatial dimension (Figure 9c). In the northern part of the Songhua River, northwestern Xinjiang and western regions are found to have negative impacts on the vegetation coverage resulting from temperature and precipitation changes. The areas where anthropogenic land use changes contributed positively to the vegetation cover account for 61.59% of the temporal dimension (Figure 9b) and 50.52% of the spatial dimension (Figure 9d). The original results (Figure 9e,f) show that the average contribution of temperature and precipitation changes to vegetation changes is 43.42% (28.41% is from the positive contribution), compared to 56.58% for anthropogenic land use changes (38.28% is from the positive contribution). Negative contributions from deforestation, desertification and urbanization are observed in the Songhua River, northern Xinjiang and southwestern China. Negative anthropogenic land use changes mainly result from the development of land, such as the expansion of farmland and built-up areas and deforestation. Overall, the contribution of temperature and precipitation changes to vegetation in mainland China are 24.73% ~ 45.56% (14.46% ~ 35.95% is from the positive contribution), and the contribution of anthropogenic land use changes to vegetation changes is 54.45% ~ 75.27% (33.54% ~ 50.52% is from the positive contribution). The contribution of anthropogenic land use changes to vegetation changes is greater than that of temperature and precipitation changes in mainland China. Anthropogenic land use changes are mainly concentrated in the eastern part (Pearl River Basin, Southeastern River, Middle and Upper Yangtze River, Middle and Lower Yangtze River, Lower Yangtze River, Huai River, Hai River, Lower Yellow River) of mainland China.

The improved methods can identify more anthropogenic land use changes impacts and negative impacts of temperature and precipitation changes (Figure 9). In terms of the temperature and precipitation changes (Figure 10a), the contribution rate ranges from −100% ~ −80%; the original method contributes 7.61%, the time dimension contributes 14.77%, and the space dimension contributes 21.69%. There is a large difference in the interval of −20% ~ 20%. The original method (13.69%) reports a similar contribution by the spatial dimension (9.65%), while the contribution of the time dimension reaches 44.19%. The contribution rate of anthropogenic land use changes (Figure 10b) varies greatly within a high range. In the range of −100% ~ −80% contribution rates, the original method contributes 6.06%, the time dimension contributes 3.88%, and the space dimension contributes 14.26%. In the range of 80% ~ 100%, the contributions of the time dimension (74.15%) and the space dimension

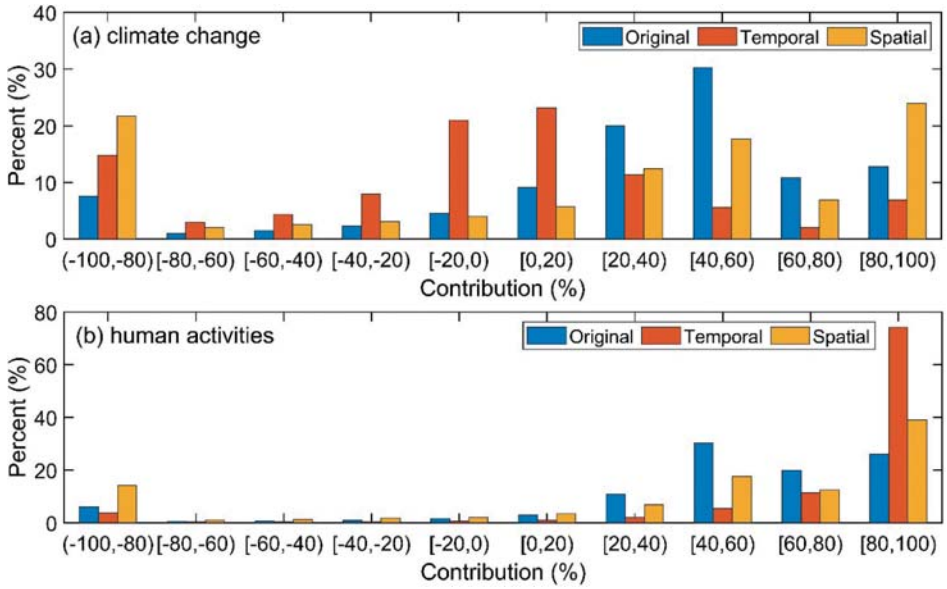


**Figure 10.** Contribution rate interval statistics of the original method and the improved method based on .Figure 9

(39.05%) are higher than those of the original method (26.09%).

The improved residual trend values provide a threshold for the rate of contribution of climate change and human activities to changes in vegetation cover that are more accurate. Improvements in the temporal dimension enhance the ability of the original residual trend method to identify the effects of human activity, while improvements in the spatial dimension reflect an underestimation of the contribution rate of the original method to climate change. An improved approach would better distinguish between the contributions of climate changes and human activities.

The smallest change in the improved results is seen in the Yellow River Basin (Upper Yellow River and Lower Yellow River) (Figure 11), where the contribution rate is essentially unchanged. The upward trend in vegetation cover is more pronounced in the Yellow River basin, where both the temperature and precipitation change and ecological engineering projects contribute to vegetation growth, so the residual trend method is better able to identify the contribution rates of both. The areas to the southwest of mainland China and the Songhua River show a large change, especially that of the Songhua River, which shows a significant increase in the contribution from changes in temperature and precipitation (10.86% ~ 20.40%) (Figure 11a,c) and a significant decrease in the contribution of ecological engineering, deforestation and urbanization (23.86% ~ 25.07%) (Figure 11b,d). This is because both regions show time lag effects on precipitation and temperature, resulting in the original residual trend method, which underestimates the vegetation's response to climate change. In addition, the modeling the spatial dimension reduces the overestimation of the contribution rate of anthropogenic land use changes due to the assumed period of no human activity.

The Middle and Lower Yangtze River, Lower Yangtze River and Southeast River present changes in the contribution rates of both the temporal and

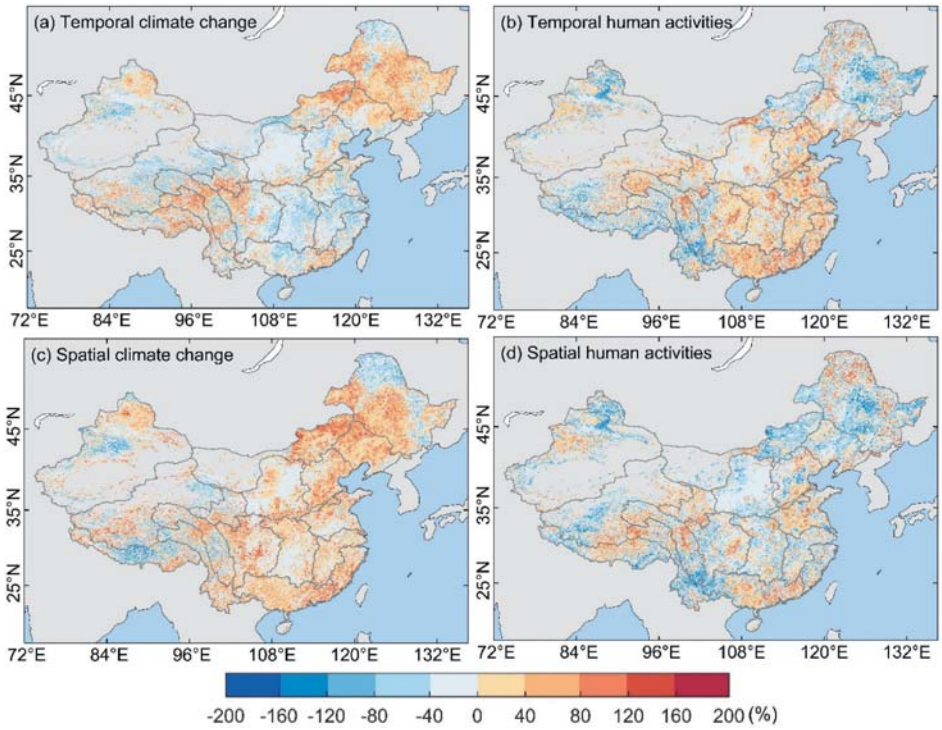


**Figure 11.** Improved results minus the results of the original residual trend method. (a) Difference in the effect of climate change between the original and improved residual trend methods in the temporal dimension. (b) Difference in the effect of human activities between the original and improved residual trend method in the temporal dimension. (c) Difference in the effect of climate change between the original and improved residual trend method in the spatial dimension. (d) Difference in the effect of human activities between the original and improved residual trend method in the spatial dimension.

spatial dimensions in addition to the opposite effect, mainly because the vegetation types in these two regions have changed significantly over time, and the use of the same vegetation type in the spatial model leads to larger errors, so the contribution rates combined with the temporal dimensions are more accurate.

Overall, the improved residual trend method provides more accurate quantitative results. It improves the ability to calculate the contribution of climate change to vegetation impacts in the temporal dimension and to identify the contribution of human activities in the spatial dimension.

The improved residual trend method provides a new threshold for the contribution of climate change and human activities to changes in vegetation based on the original method (Figure 12).

With the improvement of the residual trend method, the contribution rate of anthropogenic land use changes in the Yellow River, Yangtze River, Southeast River and Pearl River increase significantly (Figure 12a) and is more in line with the actual anthropogenic land use changes in these areas. The most prominent basin is the Lower Yellow River Basin, which accounts for 87.69% of the ecological engineering project contribution in the spatial dimension. The

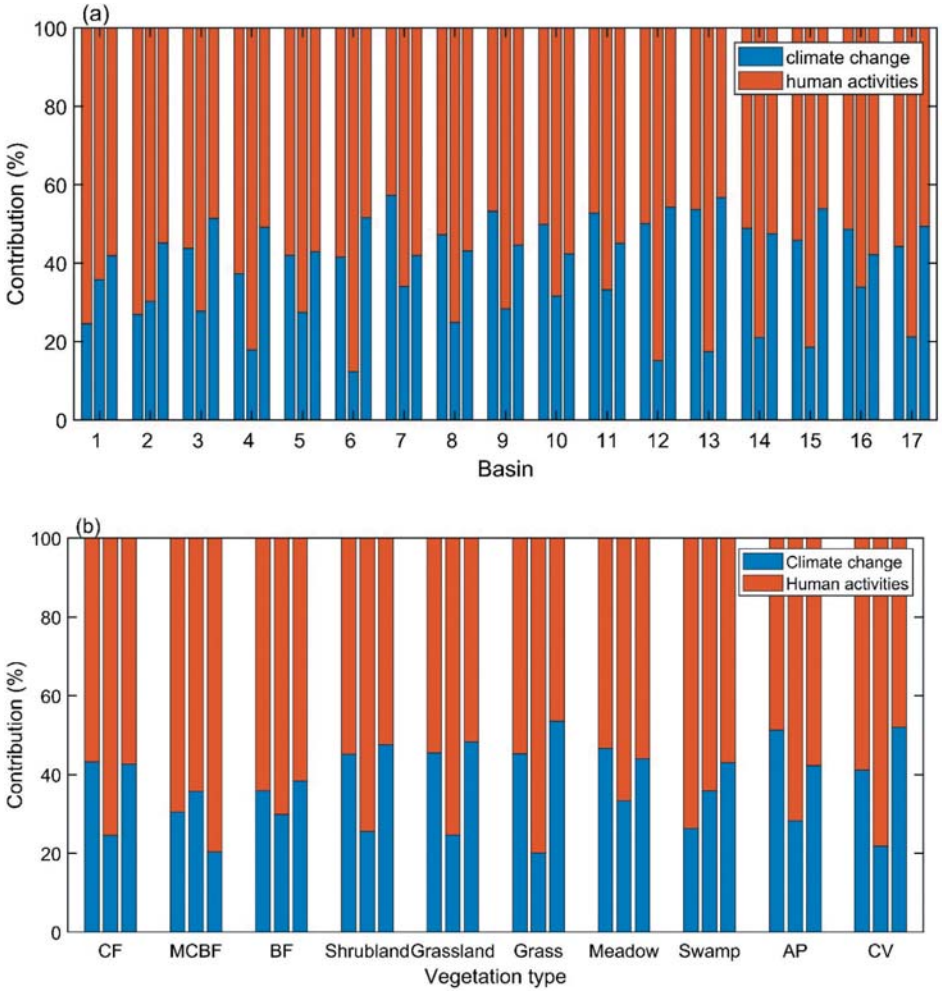


**Figure 12.** Contribution of climate change and human activities calculated from the original residual trend method and the improved residual trend method. The contribution ratio in the figure is the sum of the contribution ratios of climate change and human activities. To the left of each set of bar graphs is the original residual trend method, the middle bar shows the improved residual trend method for the spatial dimension, and the right bar represents the improved residual trend method for the temporal dimension. (a) Statistics on the contribution of climate change and human activities in the 17 basins. The names of the basins correspond to the number codes referred to in Table 1. (b) Statistics on the contribution of climate change and human activities on the 10 vegetation types. The full name of the vegetation types is referred to in Fig. 2.

negative impacts of desertification, deforestation and urbanization on vegetation are observed mainly in the Songhua River (12.67 ~ 13.58%), Upper Yangtze River (11.39% ~ 18.07%) and Lancang River (18.72% ~ 23.46%). Regarding the temperature and precipitation changes, the contribution in the temporal dimension tends to zero or greater than zero, which has a positive impact on the vegetation, while a negative impact was found on the Brahmaputra (17.42%).

Anthropogenic land use changes show a positive effect on the contribution in the temporal dimension of grass (26.49%) and CV (20.84%) vegetation types (Figure 12b). In the spatial dimension, the effect of anthropogenic land use changes on each vegetation type decreases significantly, highlighting the role of temperature and precipitation changes. The negative effects of deforestation were in the MCBF (9.53% ~ 18.76%) and BF (1.34% ~ 8.16%). The impact of the temperature and precipitation changes on vegetation is essentially positive or has no effect, but a negative impact is found in the swamp areas (33.25%) in the spatial dimension.

### 4.5. Result verification

An appropriate assessment method is a relatively important prerequisite for accurately distinguishing the impact of climate change and human activities on vegetation dynamics. In recent decades, climate change in mainland China has had great spatial heterogeneity. Overall, the temperature has increased significantly, while the spatial variation in precipitation has varied greatly (Wu et al. 2016; Zhang et al. 2019). Different vegetation types and hydrothermal conditions present in different regions lead to regional differences in vegetation change and its response to climate change (Liu et al. 2018a; Jiang et al. 2017). At the same time, the Chinese government has implemented a number of vegetation construction projects and ecological protection projects across the different regions (Xu et al. 2018b; Liu et al. 2018b), and the engineering benefits to the corresponding regions are difficult to calculate. Conversely, China's urbanization and population migration has also had a great impact on changes in the vegetation coverage (Tan, Xu, and Zhang 2016; Zhang and Shunfeng 2003). The accuracy of the RESTREND method may be significantly weakened due to the spatial heterogeneity of the vegetation-climate and vegetation-human relationships.

This research aimed to explore spatial approaches, and based on the assumption that the growth of vegetation is not disturbed by anthropogenic land use changes under the optimal hydrothermal conditions preferred by each vegetation type during the same period is necessary for the effective supplementation of the method. In the results of spatial dimension modeling, the contribution rate of anthropogenic land use change is approximately 20% lower than that of traditional time dimension modeling. In this study, it is assumed that the implications of human activities on vegetation changes before the year of abrupt change can be ignored, and the original residual trend method is further improved. However, without considering the impact of human activities in those years before the change point, the bias of the prediction equation cannot be eliminated. From the spatial dimension, we assume that under the best hydrothermal conditions, vegetation growth is not disturbed by human activities to supplement the time dimension. However, under the optimal conditions of water and heat, human activities may be influential, so the impact of temperature and precipitation changes may be overestimated. In addition, we validate our results laterally through analyzing changes in the historical land use patterns in mainland China.

Based on the 1980–2000 land use transfer matrix for mainland China (Table 4), the area converted to farmland is the largest, with a total of 1601 pixels and a net increase of 737 pixels, followed by constructed land (a net increase of 288 pixels). Grassland has the largest net reduction of 645 pixels, followed by forest areas, which showed a net reduction of 222 pixels. The land use transfer matrix in mainland China from 2000 to 2015 shows that the areas of farmland and grassland decreases, with net decreases of 94 and 320 pixels, respectively, while the net increase in constructed land is 635 pixels. From 1980 to 2015, grassland in mainland China shows an overall decreasing trend, with a net reduction of 965 pixels, mainly resulting from farmland conversion (1071 pixels of grassland were converted to farmland). In addition, the area of constructed land and farmland increased, with net increases of 921 and 643 pixels, respectively. The expansion of constructed land is mainly due to

**Table 4.** Number of pixels of land-use change in mainland China during 1980–2015.

| Land use type | Farmland | Forest | Grassland | Water | Constructed land | Unused land | Total |
|---|---|---|---|---|---|---|---|
| Number of pixels in 2000 | | | Number of pixels in 1980 | | | | |
| Farmland | - | 394 | 829 | 74 | 47 | 257 | 1601 |
| Forest | 166 | - | 265 | 17 | 3 | 30 | 481 |
| Grassland | 245 | 253 | - | 84 | 3 | 340 | 925 |
| Water | 113 | 15 | 52 | - | 1 | 87 | 268 |
| Constructed land | 276 | 11 | 30 | 16 | - | 9 | 342 |
| Unused land | 64 | 30 | 394 | 248 | 0 | - | 736 |
| Total | 864 | 703 | 1570 | 439 | 54 | 723 | 4353 |
| Number of pixels in 2015 | | | Number of pixels in 2000 | | | | |
| Farmland | - | 152 | 351 | 43 | 41 | 197 | 784 |
| Forest | 141 | - | 136 | 6 | 4 | 14 | 301 |
| Grassland | 163 | 71 | - | 25 | 1 | 137 | 397 |
| Water | 78 | 18 | 46 | - | 3 | 60 | 205 |
| Constructed land | 475 | 75 | 77 | 28 | - | 30 | 685 |
| Unused land | 21 | 6 | 107 | 41 | 1 | - | 176 |
| Total | 878 | 322 | 717 | 143 | 50 | 438 | 2548 |
| Number of pixels in 2015 | | | Number of pixels in 1980 | | | | |
| Farmland | - | 451 | 1071 | 92 | 63 | 415 | 2092 |
| Forest | 217 | - | 384 | 19 | 7 | 42 | 669 |
| Grassland | 279 | 311 | - | 95 | 4 | 444 | 1133 |
| Water | 162 | 31 | 87 | - | 4 | 118 | 402 |
| Constructed land | 732 | 84 | 108 | 38 | - | 38 | 1000 |
| Unused land | 59 | 35 | 448 | 265 | 1 | - | 808 |
| Total | 1449 | 912 | 2098 | 509 | 79 | 1057 | 6104 |

the occupation of farmland, which resulted in the conversion of 732 pixels constructed land. From 1980 to 2015, the overall distribution of land use types in mainland China are relatively stable in space, and changes are more drastic on smaller scales. The net decrease in grassland is the largest reduction, and the net increase in constructed land is the largest addition. This suggests that mainland China has experienced more human activity in recent years, which is consistent with our findings.

The Songhua River and Liao River experienced large land use changes between 1980 and 2000, especially via a drastic increase in the cultivated land. In contrast, cultivated and built-up land remain largely unchanged from 2000–2015, so fewer human activities are detected after 2000 (Figure 13). In the results of our improved residual trend method, fewer effects of human activities are detected in the Songhua River Basin and the Liao River than in the original method. The improved residual trend method detected a higher anthropogenic contribution than the original method in the Upper Yellow River, Huai River, Inland rivers in Northern Tibet, Brahmaputra, Upper and Middle Yangtze River and Lancang River. The Upper Yellow River, Huai River, and Upper and Middle Yangtze River show significantly increased areas with constructed land, while Inland rivers in Northern Tibet (0.044% to 0.12%), Brahmaputra (0.034% to 0.068%), Upper Yangtze River (0.14% to 0.27%) and Lancang River (0.17% to 0.25%) are difficult to see in the figure due to their relatively small proportions of constructed land; however, their constructed land area has basically doubled.

Compared with previous studies, our results are consistent and reasonable (Huang et al. 2020; Jiang et al., 2020; Liu et al. 2018a; Sun et al. 2015b; Wang et al. 2013). In the temporal dimension, the ability to identify the effects of temperature and precipitation changes on vegetation change is enhanced by our method; in the spatial dimension, the rate of contribution of anthropogenic land use changes to vegetation change is highlighted. Combining the results of both makes the residual trend method more accurate. Changes in the vegetation coverage in most parts of China is caused by human activities and climate change factors. Overall, the contributions of temperature and precipitation changes and anthropogenic land use changes are approximately 40% and 60% (Kai. 2019), respectively, from our results. According to the results of some regions, anthropogenic land use changes contributed to 42.35% and temperature and precipitation changes contributed to 57.65% of the vegetation change in the Loess Plateau from 2000 to 2016 (Zheng et al. 2019b). The contribution of human activities to vegetation changes on the Loess Plateau was 55% from 1982 to 2015 (Li, Peng, and Li 2017). Our research shows that climate change and human activities accounted for 48.94% ~ 62.98% and 37.02% ~ 51.06% of the vegetation changes seen in the Yellow River (including the Upper Yellow River

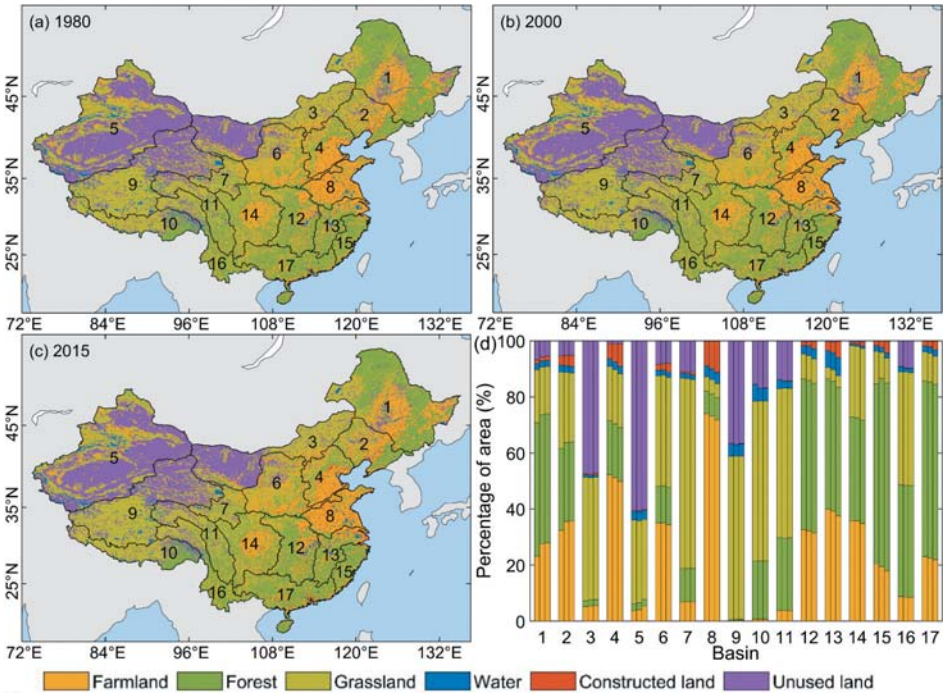


**Figure 13.** Spatial distribution of the historical land use types in mainland China. (a) Status of land use in 1980. (b) Status of land use in 2000. (c) Status of land use in 2015. (d) Proportion of land use types in 17 basins in 1980, 2000, and 2015 (the left column is 1980; the middle column is 2000; and the right column is 2015).

and Lower Yellow River, which contains the Loess Plateau) from 1982 to 2015, which is similar to the results of previous research but more accurate. Another study showed that the relative contributions of temperature and precipitation changes and anthropogenic land use changes accounted for 46.6% and 53.4% in arid and semiarid areas of China, respectively, from 1983 to 2012 (Feng et al. 2015). From Figure 8, the range of influence of climate change and human activities to NDVI is similar in arid and semiarid areas coinciding with the results of the compared research. Overall, the improved residual trend method further refines the theory of the impact of the temporal dimension, establishes the nonlinear relationship between NDVI and climate factors, considers time-lagged effects and sets up a hypothetical anthropogenic-free period. However, the anthropogenic bias of the NDVI assumptions cannot be eliminated, so this study adds a spatial dimension, i.e., a spatially simulated equation, at the same time, assuming that the vegetation is not affected by human activities under optimal thermal and hydrothermal conditions. The improvement in the spatial dimension can negate the bias introduced in the temporal dimension, but it does not completely exclude the new bias introduced by anthropogenic influences at optimal hydrothermal conditions. We, therefore, provide a threshold reference for the contribution of climate change and human activities to vegetation changes. We believe that our research further improved the residual trend method and obtained more accurate results.

## 5. Conclusions

Anthropogenic land use changes and temperature and precipitation changes are the two main factors driving changes in vegetation cover on regional and global scales. This paper improves the residual trend method to determine the contribution rate of anthropogenic land use changes in the temporal and spatial dimensions on the basis of ensuring a more accurate quantification of the temperature and precipitation change contribution rates to the actual NDVI values. Taking mainland China as a research object from 1982 to 2015, we concluded the following: (1) 68.81% of the area is in a state of sustainable increase in vegetation coverage, of which the cultivated vegetation (CV) and grass components are dominant. (2) The contribution of temperature and precipitation to vegetation

is 24.73% ~ 45.56%; the contribution rate of anthropogenic land use changes to changes in vegetation is 54.45% ~ 75.27%. (3) The improved residual trend method enhances the accuracy of the calculated contribution rates of climate change and human activities to vegetation changes in the temporal and spatial dimensions, respectively. (4) Although increasing attention has been given to the effect of anthropogenic land use changes on vegetation changes, we cannot ignore the impact of temperature and precipitation changes.

## Disclosure statement

No potential conflict of interest was reported by the authors.

## Funding

This study was supported by the National Key Research and Development Program of China [No. 2018YFE0196000], the Second Tibetan Plateau Scientific Expedition and Research Program [No. 2019QZKK0405], and the Natural Science Foundation of China [No. 51879009].

## References

Bai, Y., Y. Yang, and H. Jiang. 2019. "Intercomparison of AVHRR GIMMS3g, Terra MODIS, and SPOT-VGT NDVI Products over the Mongolian Plateau." *Remote Sensing* 11 (17): 2030. doi:10.3390/rs11172030.

Bao, G., Z. Qin, Y. Bao, Y. Zhou, W. Li, and A. Sanjjav. 2014. "NDVI-based Long-term Vegetation Dynamics and Its Response to Climatic Change in the Mongolian Plateau." *Remote Sensing* 6 (9): 8337–8358. doi:10.3390/rs6098337.

Beck, H. E., T. R. McVicar, A. I. J. M. van Dijk, J. Schellekens, R. A. M. de Jeu, and L. A. Bruijnzeel. 2011. "Global Evaluation of Four AVHRR–NDVI Data Sets: Intercomparison and Assessment against Landsat Imagery." *Remote Sensing of Environment* 115 (10): 2547–2563. doi:10.1016/j.rse.2011.05.012.

Bégué, A., E. Vintrou, D. Ruelland, M. Claden, and N. Dessay. 2011. "Can A 25-year Trend in Soudano-Sahelian Vegetation Dynamics Be Interpreted in Terms of Land Use Change? A Remote Sensing Approach." *Global Environmental Change* 21 (2): 413–420. doi:10.1016/j.gloenvcha.2011.02.002.

Bonan, G. B. 2008. "Forests and Climate Change: Forcings, Feedbacks, and the Climate Benefits of Forests." *Science* 320 (5882): 1444–1449. doi:10.1126/science.1155121.

Burrell, A. L., J. P. Evans, and Y. Liu. 2017. "Detecting Dryland Degradation Using Time Series Segmentation and Residual Trend Analysis (Tss-restrend)." *Remote Sensing of Environment* 197: 43–57. doi:10.1016/j.rse.2017.05.018.

Cai, T. T., and P. Hall. 2006. "Prediction in Functional Linear Regression." *Annals of Statistics* 34 (5): 2159–2179. doi:10.1214/009053606000000830.

Chen, B., G. Xu, N. C. Coops, P. Ciais, J. L. Innes, G. Wang, … L. Cao. 2014. "Changes in Vegetation Photosynthetic Activity Trends across the Asia–Pacific Region over the Last Three Decades." *Remote Sensing of Environment* 144: 28–41. doi:10.1016/j.rse.2013.12.018.

Chen, C., T. Park, X. Wang, S. Piao, B. Xu, R. K. Chaturvedi, … H. Tømmervik. 2019. "China and India Lead in Greening of the World through Land-use Management." *Nature Sustainability* 2 (2): 122. doi:10.1038/s41893-019-0220-7.

Chen, X., B. Hu, and R. Yu. 2005. "Spatial and Temporal Variation of Phenological Growing Season and Climate Change Impacts in Temperate Eastern China." *Global Change Biology* 11 (7): 1118–1130. doi:10.1111/j.13652486.2005.00974.x.

Churkina, G., and S. W. Running. 1998. "Contrasting Climatic Controls on the Estimated Productivity of Global Terrestrial Biomes." *Ecosystems* 1 (2): 206–215. doi:10.1007/s100219900016.

Cui, J., S. Piao, C. Huntingford, X. Wang, X. Lian, A. Chevuturi, A. G. Turner, and G. J. Kooperman. 2020. "Vegetation Forcing Modulates Global Land Monsoon and Water Resources in a CO 2 -enriched Climate." *Nature Communications* 11 (1): 5184. doi:10.1038/s41467-020-18992-7.

de Jong, R., S. de Bruin, A. de Wit, M. E. Schaepman, and D. L. Dent. 2011. "Analysis of Monotonic Greening and Browning Trends from Global NDVI Time-series." *Remote Sensing of Environment* 115 (2): 692–702. doi:10.1016/j.rse.2010.10.011.

Deng, X., J. Huang, S. Rozelle, J. Zhang, and Z. Li. 2015. "Impact of Urbanization on Cultivated Land Changes in China." *Land Use Policy* 45 (45): 1–7. doi:10.1016/j.landusepol.2015.01.007.

Du, J., Q. Fu, S. Fang, J. Wu, P. He, and Z. Quan. 2019. "Effects of Rapid Urbanization on Vegetation Cover in the Metropolises of China over the Last Four Decades." *Ecological Indicators* 107: 105458. doi:10.1016/j.ecolind.2019.105458.

Evans, J., and R. Geerken. 2004. "Discrimination between Climate and Human-induced Dryland Degradation." *Journal of Arid Environments* 57: 535–554. doi:10.1016/S0140-1963(03)00121-6.

Faour, G., M. Mhawej, and A. Nasrallah. 2018. "Global Trends Analysis of the Main Vegetation Types Throughout the past Four Decades." *Applied Geography* 97: 184–195. doi:10.1016/j.ecolind.2018.11.037.

Fatima, Z., M. Ahmed, M. Hussain, G. Abbas, S. Ul-Allah, S. Ahmad, N. Ahmed, et al. 2020. "The Fingerprints of Climate Warming on Cereal Crops Phenology and Adaptation Options." *Scientific Reports* 10 (1): 18013. doi:10.1038/s41598-020-74740-3.

Feng, Q., H. Ma, X. Jiang, X. Wang, and S. Cao. 2015. "What Has Caused Desertification in China?" *Scientific Reports* 5: 15998. doi:10.1038/srep15998.

Fensholt, R., and S. R. Proud. 2012. "Evaluation of Earth Observation Based Global Long Term Vegetation trends—

Comparing GIMMS and MODIS Global NDVI Time Series." *Remote Sensing of Environment* 119: 131–147. doi:10.1016/j.rse.2011.12.015.

Foley, J. A., S. Levis, M. H. Costa, W. Cramer, and D. Pollard. 2000. "Incorporating Dynamic Vegetation Cover within Global Climate Models." *Ecological Applications* 10 (6): 1620–1632. doi:10.1890/1051-0761(2000)010[1620:IDVCWG]2.0.CO;2.

Gong, D. Y., Y. Z. Pan, and J. A. Wang. 2004. "Changes in Extreme Daily Mean Temperatures in Summer in Eastern China during 1955–2000." *Theoretical and Applied Climatology* 77 (1–2): 25–37. doi:10.1007/s00704-003-0019-2.

Gu, Y., B. K. Wylie, D. M. Howard, K. P. Phuyal, and L. Ji. 2013. "NDVI Saturation Adjustment: A New Approach for Improving Cropland Performance Estimates in the Greater Platte River Basin, USA." *Ecological Indicators* 30: 1–6. doi:10.1016/j.ecolind.2013.01.041.

Guo, L., S. Wu, D. Zhao, Y. Yin, G. Leng, and Q. Zhang. 2014. "NDVI-based Vegetation Change in Inner Mongolia from 1982 to 2006 and Its Relationship to Climate at the Biome Scale." *Advances in Meteorology* 2014. doi:10.1155/2014/692068.

Higginbottom, T. P., and E. Symeonakis. 2014. "Assessing Land Degradation and Desertification Using Vegetation Index Data: Current Frameworks and Future Directions." *Remote Sensing* 6 (10): 9552–9575. doi:10.3390/rs6109552.

Hilker, T., E. Natsagdorj, R. H. Waring, A. Lyapustin, and Y. Wang. 2014. "Satellite Observed Widespread Decline in Mongolian Grasslands Largely Due to Overgrazing." *Global Change Biology* 20 (2): 418–428. doi:10.1111/gcb.12365.

Holben, and N. Brent. 2007. "Characteristics of Maximum-value Composite Images from Temporal AVHRR Data." *International Journal of Remote Sensing* 7: 1417–1434. doi:10.1080/01431168608948945.

Hou, X. Y. 2001. *Vegetation Atlas of China (1:1000000)*. Beijing: Science Press.

Hua, W., and H. Chen. 2013. "Recognition of Climatic Effects of Land Use/land Cover Change under Global Warming." *Chinese Science Bulletin* 58 (31): 3852–3858. doi:10.1007/s11434-013-5902-3.

Hua, W., H. Chen, L. Zhou, Z. Xie, M. Qin, X. Li, … S. Sun. 2017. "Observational Quantification of Climatic and Human Influences on Vegetation Greening in China." *Remote Sensing* 9 (5): 425. doi:10.3390/rs9050425.

Huang, S., X. Zheng, L. Ma, H. Wang, Q. Huang, G. Leng, E. Meng, and Y. Guo. 2020. "Quantitative Contribution of Climate Change and Human Activities to Vegetation Cover Variations Based on GA-SVM Model." *Journal of Hydrology* 584: 124687. doi:10.1016/j.jhydrol.2020.124687.

Huete, A., C. Justice, and W. Van Leeuwen. 1999. "MODIS Vegetation Index (MOD13)." *Algorithm Theoretical Basis Document* 3. https://modis.gsfc.nasa.gov/data/atbd/atbd_mod13.pdf

Ibrahim, Y. Z., H. Balzter, J. Kaduk, and C. J. Tucker. 2015. "Land Degradation Assessment Using Residual Trend Analysis of GIMMS NDVI3g, Soil Moisture and Rainfall in Sub-Saharan West Africa from 1982 to 2012." *Remote Sensing* 7 (5): 5471–5494. doi:10.3390/rs70505471.

Jiang, H., X. Xu, M. Guan, L. Wang, Y. Huang, and Y. Jiang. 2019. "Determining the Contributions of Climate Change and Human Activities to Vegetation Dynamics in Ago-pastural Transitional Zone of Northern China from 2000 to 2015." *Science of the Total Environment* 134871. doi:10.1016/j.scitotenv.2019.134871.

Jiang, L., A. Bao, H. Guo, and F. Ndayisaba. 2017. "Vegetation Dynamics and Responses to Climate Change and Human Activities in Central Asia." *Science of the Total Environment* 599: 967–980. doi:10.1016/j.scitotenv.2017.05.012.

Jiyuan, Z., Qian, and Yunfeng. 2012. "Regional differences of china□s urban expansion from late 20th to early 21st century based on remote sensing information." *Chinese Geographical Science* 22 (1): 1–14. doi:10.1007/s11769-012-0510-8.

Kai., J. 2019. "Spatio-temporal Variations of Vegetation Cover and Its Relationships between Climate Change and Human Activities over China." Ph.D. Thesis, Northwest A□F University, China.

Kawabata, A., K. Ichii, and Y. Yamaguchi. 2001. "Global Monitoring of Interannual Changes in Vegetation Activities Using Ndvi and Its Relationships to Temperature and Precipitation." *International Journal of Remote Sensing* 22 (7): 1377–1382. doi:10.1080/01431160119381.

Kong, D., C. Miao, J. Wu, H. Zheng, and S. Wu. 2020. "Time Lag of Vegetation Growth on the Loess Plateau in Response to Climate Factors: Estimation, Distribution, and Influence." *Science of the Total Environment* 744: 140726. doi:10.1016/j.scitotenv.2020.140726.

Lamchin, M., W. K. Lee, S. W. Jeon, S. W. Wang, C. H. Lim, C. Song, and M. Sung. 2018. "Long-term Trend and Correlation between Vegetation Greenness and Climate Variables in Asia Based on Satellite Data." *Science of the Total Environment* 618: 1089–1095. doi:10.1016/j.scitotenv.2017.09.145.

Lang, Y., A. Ye, W. Gong, C. Miao, Z. Di, J. Xu, Y. Liu, L. Luo, and Q. Duan. 2014. "Evaluating Skill of Seasonal Precipitation and Temperature Predictions of NCEP CFSv2 Forecasts over 17 Hydroclimatic Regions in China." *Journal of Hydrometeorology* 15 (4): 1546–1559. doi:10.1175/JHM-D-13-0208.1.

Li, J., S. Peng, and Z. Li. 2017. "Detecting and Attributing Vegetation Changes on China's Loess Plateau." *Agricultural and Forest Meteorology* 247: 260–270. doi:10.1016/j.agrformet.2017.08.005.

Li, X. B., R. H. Li, G. Q. Li, H. Wang, Z. F. Li, X. Li, and X. Y. Hou. 2016. "Human-induced Vegetation Degradation and Response of Soil Nitrogen Storage in Typical Steppes in Inner Mongolia, China." *Journal of Arid Environments* 124: 80–90. doi:10.1016/j.jaridenv.2015.07.013.

Liu, C., J. Melack, Y. Tian, H. Huang, J. Jiang, X. Fu, and Z. Zhang. 2019. "Detecting Land Degradation in Eastern China Grasslands with Time Series Segmentation and Residual Trend Analysis (TSS-RESTREND) and GIMMS NDVI3g Data." *Remote Sensing* 11 (9): 1014. doi:10.3390/rs11091014.

Liu, J., and P. H. Raven. 2010. "China\"s Environmental Challenges and Implications for the World." *Critical Reviews in Environmental Science and Technology* 40 (9–10): 823–851. doi:10.1080/10643389.2010.502645.

Liu, R., L. Xiao, Z. Liu, and J. Dai. 2018. "Quantifying the Relative Impacts of Climate and Human Activities on Vegetation Changes at the Regional Scale." *Ecological Indicators* 93: 91–99. doi:10.1016/j.ecolind.2018.04.047.

Liu, X. F., X. F. Zhu, Y. Z. Pan, Y. Z. Li, and A. Z. Zhao. 2015. "Spatiotemporal Changes in Vegetation Coverage in China during 1982–2012." *Acta Ecologica Sinica* 35: 5331–5342. doi:10.5846/stxb201404150731.

Liu, Z., Y. Liu, and Y. Li. 2018. "Anthropogenic Contributions Dominate Trends of Vegetation Cover Change over the Farming-pastoral Ecotone of Northern China." *Ecological Indicators* 95: 370–378. doi:10.1016/j.ecolind.2018.07.063.

Ma, F., A. Ye, X. Deng, Z. Zhou, X. Liu, Q. Duan, J. Xu, C. Miao, Z. Di, and W. Gong. 2016. "Evaluating the Skill of NMME Seasonal Precipitation Ensemble Predictions for 17 Hydroclimatic Regions in Continental China." *International Journal of Climatology* 36 (1): 132–144. doi:10.1002/joc.4333.

Ma, F., A. Ye, J. You, and Q. Duan. 2018. "2015–16 Floods and Droughts in China, and Its Response to the Strong El Niño." *Science of the Total Environment* 627: 1473–1484. https://doi.org/10.1016/j.scitotenv.2018.01.280.

Ma, F., X. Yuan, and A. Ye. 2015. "Seasonal Drought Predictability and Forecast Skill over China." *Journal of Geophysical Research: Atmospheres* 120 (16): 8264–8275. doi:10.1002/2015JD023185.

Mao, D., Z. Wang, L. Luo, and C. Ren. 2012. "Integrating AVHRR and MODIS Data to Monitor NDVI Changes and Their Relationships with Climatic Parameters in Northeast China." *International Journal of Applied Earth Observation and Geoinformation* 18: 528–536. doi:10.1016/j.jag.2011.10.007.

Menzel, A., T. H. Sparks, N. Estrella, E. Koch, A. Aasa, R. Ahas, … F. M. Chmielewski. 2006. "European Phenological Response to Climate Change Matches the Warming Pattern." *Global Change Biology* 12 (10): 1969–1976. doi:10.1111/j.1365-2486.2006.01193.x.

Mu, S., S. Zhou, Y. Chen, J. Li, W. Ju, and I. O. A. Odeh. 2013. "Assessing the Impact of Restoration-induced Land Conversion and Management Alternatives on Net Primary Productivity in Inner Mongolian Grassland, China." *Global and Planetary Change* 108: 29–41. doi:10.1016/j.gloplacha.2013.06.007.

Neigh, C. S., C. J. Tucker, and J. R. Townshend. 2008. "North American Vegetation Dynamics Observed with Multi-resolution Satellite Data." *Remote Sensing of Environment* 112 (4): 1749–1772. doi:10.1016/j.rse.2007.08.018.

Nemani, R. R., C. D. Keeling, H. Hashimoto, W. M. Jolly, S. C. Piper, C. J. Tucker, … S. W. Running. 2003. "Climate-driven Increases in Global Terrestrial Net Primary Production from 1982 to 1999." *science* 300 (5625): 1560–1563. doi:10.1126/science.1082750.

Pan, T., X. Zou, Y. Liu, S. Wu, and G. He. 2017. "Contributions of Climatic and Non-climatic Drivers to Grassland Variations on the Tibetan Plateau." *Ecological Engineering* 108: 307–317. doi:10.1016/j.ecoleng.2017.07.039.

Peel, M. C., B. L. Finlayson, and T. A. McMahon. 2007. "Updated World Map of the Köppen-Geiger Climate Classification." *Hydrology and Earth System Sciences* 11: 1633–1644. doi:10.5194/hess-11-1633-2007.

Peng, S., A. Chen, L. Xu, C. Cao, J. Fang, R. B. Myneni, J. E. Pinzon, C. J. Tucker, and S. Piao. 2011. "Recent Change of Vegetation Growth Trend in China." *Environmental Research Letters* 6: 044027. doi:10.1088/1748-9326/6/4/044027.

Pettitt, A. N. 1979. "A Non-parametric Approach to the Change-point Problem." *Journal of the Royal Statistical Society: Series C (Applied Statistics)* 28 (2): 126–135. doi:10.2307/2346729.

Pettorelli, N., J. O. Vik, A. Mysterud, J. M. Gaillard, C. J. Tucker, and N. C. Stenseth. 2005. "Using the Satellite-derived NDVI to Assess Ecological Responses to Environmental Change." *Trends in Ecology & Evolution* 20 (9): 503–510. doi:10.1016/j.tree.2005.05.011.

Piao, S., G. Yin, J. Tan, L. Cheng, M. Huang, Y. Li, R. Liu, et al. 2015. "Detection and Attribution of Vegetation Greening Trend in China over the Last 30 Years." *Global Change Biology* 21: 1601–1609. doi:10.1111/gcb.12795.

Pinzon, J., and C. Tucker. 2014. "A Non-Stationary 1981–2012 AVHRR NDVI3g Time Series." *Remote Sensing* 6: 6929–6960. doi:10.3390/rs6086929.

Qian, W., and X. Lin. 2005. "Regional Trends in Recent Precipitation Indices in China." *Meteorology and Atmospheric Physics* 90 (3–4): 193–207. doi:10.1007/s00703-004-0101-z.

Ramsay, J. O. 1977. "A Comparative Study of Several Robust Estimates of Slope, Intercept, and Scale in Linear Regression." *Journal of the American Statistical Association* 72 (359): 608–615. doi:10.1080/01621459.1977.10480624.

Ren, G., J. Guo, M. Z. Xu, Z. Y. Chu, L. Zhang, X. K. Zou, Q. Li, and X. N. Liu. 2005. "Climate Changes of Mainland China over the past Half Century." *Acta Meteorologica Sinica* 63: 942–956.

Schultz, P. A., and M. S. Halpert. 1993. "Global Correlation of Temperature, Ndvi and Precipitation." *Advances in Space Research* 13 (5): 277–280. doi:10.1016/0273-1177(93)90559-T.

Schuur, E. A. G. 2003. "Productivity and Global Climate Revisited: The Sensitivity of Tropical Forest Growth to Precipitation." *Ecology* 84 (5): 1165–1170. doi:10.2307/3107925.

Shi, C., Z.-H. Jiang, W.-L. Chen, and L. Li. 2018. "Changes in Temperature Extremes over China under 1.5 °C and 2 °C Global Warming Targets." *Advances in Climate Change Research* 9 (2): 120–129. doi:10.1016/j.accre.2017.11.003.

Slayback, D. A., J. E. Pinzon, S. O. Los, and C. J. Tucker. 2003. "Northern Hemisphere Photosynthetic Trends 1982–99." *Global Change Biology* 9 (1): 1–15. doi:10.1046/j.1365-2486.2003.00507.x.

Son, N. T., C. F. Chen, C. R. Chen, V. Q. Minh, and N. H. Trung. 2014. "A Comparative Analysis of Multitemporal MODIS EVI and NDVI Data for Large-scale Rice Yield Estimation."

*Agricultural and Forest Meteorology* 197: 52–64. doi:10.1016/j.agrformet.2014.06.007.

Sun, W., X. Song, X. Mu, P. Gao, F. Wang, and G. Zhao. 2015a. "Spatiotemporal Vegetation Cover Variations Associated with Climate Change and Ecological Restoration in the Loess Plateau." *Agricultural and Forest Meteorology* 209: 87–99. doi:10.1016/j.agrformet.2015.05.002.

Sun, Y. 2012. "Variation of Vegetation Coverage and Its Relationship with Climate Change in North China from 1982 to 2006." *Ecology & Environmental Sciences* 21: 7–12. doi:10.3969/j..1674-5906.2012.01.002.

Sun, Y., Y. Yang, L. Zhang, and Z. Wang. 2015b. "The Relative Roles of Climate Variations and Human Activities in Vegetation Change in North China." *Physics and Chemistry of the Earth Parts A/B/C* 87: 67–78. doi:10.1016/j.pce.2015.09.017.

Tan, Y., H. Xu, and X. Zhang. 2016. "Sustainable Urbanization in China: A Comprehensive Literature Review." *Cities* 55: 82–93. doi:10.1016/j.cities.2016.04.002.

Testa, S., K. Soudani, L. Boschetti, and E. Borgogno Mondino. 2018. "MODIS-derived EVI, NDVI and WDRVI Time Series to Estimate Phenological Metrics in French Deciduous Forests." *International Journal of Applied Earth Observation and Geoinformation* 64: 132–144. doi:10.1016/j.jag.2017.08.006.

Tian, G. J., D. F. Zhuang, and M. L. Liu. 2003. "The Spatial-temporal Dynamic Change of Cultivated Land in China in 1990s." *Advance in Earth Sciences* 18 (1): 30–036. doi:10.11867/j..1001-8166.2003.01.0030.

Tong, X., K. Wang, Y. Yue, M. Brandt, B. Liu, C. Zhang, ... & Fensholt, R. 2017. "Quantifying the Effectiveness of Ecological Restoration Projects on Long-term Vegetation Dynamics in the Karst Regions of Southwest China." *International Journal of Applied Earth Observation and Geoinformation* 54 :105–113. doi:10.1016/j.jag.2016.09.013.

Tucker, C. J., B. N. Holben, and T. E. Goff. 1984. "Intensive Forest Clearing in Rondonia, Brazil, as Detected by Satellite Remote Sensing." *Remote Sensing of Environment* 15 (3): 255–261. doi:10.1016/0034-4257(84)90035-X.

Wang, F., X. Pan, D. Wang, C. Shen, and Q. Lu. 2013. "Combating Desertification in China: Past, Present and Future." *Land Use Policy* 31 (none). doi:10.1016/j.landusepol.2012.07.010.

Wang, G., and L. Han, 2012. "The Vegetation NDVI Variation Trend in Qinghai-Tibet Plateau and Its Response to Climate Change." 2nd International Conference on Remote Sensing, Environment and Transportation Engineering (RSETE) - Nanjing, Jiangsu, China (2012.06.1-2012.06.3). Q17 IEEE, 1–4. doi:10.1109/RSETE.2012.6260792

Wang, J., P. M. Rich, and K. P. Price. 2003. "Temporal Responses of Ndvi to Precipitation and Temperature in the Central Great Plains, Usa." *International Journal of Remote Sensing* 24 (11): 2345–2364. doi:10.1080/01431160210154812.

Wang, J., K. Wang, M. Zhang, and C. Zhang. 2015. "Impacts of Climate Change and Human Activities on Vegetation Cover in Hilly Southern China." *Ecological Engineering* 81: 451–461. doi:10.1016/j.ecoleng.2015.04.022.

Wu, D., X. Zhao, S. Liang, T. Zhou, K. Huang, B. Tang, and W. Zhao. 2015. "Time-lag Effects of Global Vegetation Responses to Climate Change." *Global Change Biology* 21: 3520–3531. doi:10.1111/gcb.12945.

Wu, Y., S. Y. Wu, J. Wen, M. Xu, and J. Tan. 2016. "Changing Characteristics of Precipitation in China during 1960-2012." *International Journal of Climatology* 36 (3): 1387–1402. doi:10.1002/joc.4432.

Wu, Z., J. Wu, J. Liu, B. He, T. Lei, and Q. Wang. 2013. "Increasing Terrestrial Vegetation Activity of Ecological Restoration Program in the Beijing–Tianjin Sand Source Region of China." *Ecological Engineering* 52: 37–50. doi:10.1016/j.ecoleng.2012.12.040.

Xie, B., X. Jia, Z. Qin, J. Shen, and Q. Chang. 2015. "Vegetation Dynamics and Climate Change on the Loess Plateau, China: 1982–2011." *Regional Environmental Change* 16 (6): 1–12. doi:10.1007/s10113-015-0881-3.

Xu, G., H. Zhang, B. Chen, H. Zhang, J. Innes, G. Wang, … R. Myneni. 2014. "Changes in Vegetation Growth Dynamics and Relations with Climate over China's Landmass from 1982 to 2011." *Remote Sensing* 6 (4): 3263–3283. doi:10.3390/rs6043263.

Xu, H. J., X. P. Wang, and T. B. Yang. 2017. "Trend Shifts in Satellite-derived Vegetation Growth in Central Eurasia, 1982–2013." *Science of the Total Environment* 579: 1658–1674. doi:10.1016/j.scitotenv.2016.11.182.

Xu, G., J. Zhang, P. Li, Z. Li, K. Lu, X. Wang, … B. Wang. 2018a. "Vegetation Restoration Projects and Their Influence on Runoff and Sediment in China." *Ecological Indicators* 95: 233–241. doi:10.1016/j.ecolind.2018.07.047.

Xu, L., Z. Tu, Y. Zhou, and G. Yu. 2018b. "Profiling Human-Induced Vegetation Change in the Horqin Sandy Land of China Using Time Series Datasets." *Sustainability* 10 (4): 1068. doi:10.3390/su10041068.

Xu, X., Y. Du, J. Tang, and Y. Wang. 2011. "Variations of Temperature and Precipitation Extremes in Recent Two Decades over China." *Atmospheric Research* 101 (1–2): 143–154. doi:10.1016/j.atmosres.2011.02.003.

Ying, Z. 2012. "Projections of 2.0°C Warming over the Globe and China under RCP4.5." *Atmospheric and Oceanic Science Letters* 5 (6): 514–520. doi:10.1080/16742834.2012.11447047.

Zhai, P., X. Zhang, H. Wan, and X. Pan. 2005. "Trends in Total Precipitation and Frequency of Daily Precipitation Extremes over China." *Journal of Climate* 18 (7): 1096–1108. doi:10.1175/JCLI-3318.1.

Zhai, and Panmao. 2003. "Trends in Temperature Extremes during 1951–1999 in China." *Geophysical Research Letters* 30 (17): 1913. doi:10.1029/2003gl018004.

Zhang, G., T. Yao, W. Chen, G. Zheng, C. K. Shum, K. Yang, … C. M. O'Reilly. 2019. "Regional Differences of Lake Evolution across China during 1960s–2015 and Its Natural and Anthropogenic Causes." *Remote Sensing of Environment* 221: 386–404. doi:10.1016/j.rse.2018.11.038.

Zhang, K. H., and S. Shunfeng. 2003. "Rural–urban Migration and Urbanization in China: Evidence from Time-series and

Cross-section Analyses." *China Economic Review* 14 (4): 386–400. doi:10.1016/j.chieco.2003.09.018.

Zhang, Y., and A. Ye. 2020. "Spatial and Temporal Variations in Vegetation Coverage Observed Using AVHRR GIMMS and Terra MODIS Data in the Mainland of China." *International Journal of Remote Sensing* 41 (11): 4238–4268. doi:10.1080/01431161.2020.1714781.

Zhang, Y., C. Zhang, Z. Wang, Y. Chen, C. Gang, R. An & Li, J. 2016. "Vegetation Dynamics and Its Driving Forces from Climate Change and Human Activities in the Three-river Source Region, China from 1982 to 2012." *Science of the Total Environment* 563-564 :210–220. doi:10.1016/j.scitotenv.2016.03.223.

Zhao, J., S. Huang, Q. Huang, H. Wang, G. Leng, and W. Fang. 2020. "Time-lagged Response of Vegetation Dynamics to Climatic and Teleconnection Factors." *CATENA* 189: 104474. doi:10.1016/j.catena.2020.104474.

Zheng, D., G. Shi, S. R. Hemming, H. Zhang, W. Wang, B. Wang, and S.-C. Chang. 2019a. "Age Constraints on a Neogene Tropical Rainforest in China and Its Relation to the Middle Miocene Climatic Optimum." *Palaeogeography, Palaeoclimatology, Palaeoecology* 518: 82–88. doi:10.1016/j.palaeo.2019.01.019.

Zheng, K., J. Z. Wei, J. Y. Pei, H. Cheng, X. L. Zhang, F. Q. Huang, … J. S. Ye. 2019b. "Impacts of Climate Change and Human Activities on Grassland Vegetation Variation in the Chinese Loess Plateau." *Science of the Total Environment* 660: 236–244. doi:10.1016/j.scitotenv.2019.01.022.

Zhou, D., S. Zhao, and C. Zhu. 2012. "The Grain for Green Project Induced Land Cover Change in the Loess Plateau: A Case Study with Ansai County, Shanxi Province, China." *Ecological Indicators* 23 (none): 0–94. doi:10.1016/j.ecolind.2012.03.021.

Zhou, X., Y. Yamaguchi, and S. Arjasakusuma. 2018. "Distinguishing the Vegetation Dynamics Induced by Anthropogenic Factors Using Vegetation Optical Depth and AVHRR NDVI: A Cross-border Study on the Mongolian Plateau." *Science of the Total Environment* 616–617: 730–743. doi:10.1016/j.scitotenv.2017.10.253.

Zhou, X. X., Y. H. Ding, and P. X. Wang. 2010. "Moisture Transport in Asian Summer Monsoon Region and Its Relationship with Summer Precipitation in China." *Journal of Meteorological Research* 24 (1): 31–42. doi:10.3724/SP.J.1047.2008.00014.

Zhu, H. 2013. "Geographical Elements of Seed Plants Suggest the Boundary of the Tropical Zone in China." *Palaeogeography, Palaeoclimatology, Palaeoecology* 386: 16–22. doi:10.1016/j.palaeo.2013.04.007.

## Appendix

The annual average temperature in mainland China increased significantly from 1982–2015, especially from 1982–2000 (Figure A1). The annual total precipitation fluctuated greatly from 1982 to 2015, but the overall change was not significant (Figure A2). Most of the temperature measurements in mainland China from 1982 to 2015 showed a clear upward trend (Figure A3). There are large spatial differences in the precipitation trends in mainland China seen from 1982 to 2015 (Figure A4).

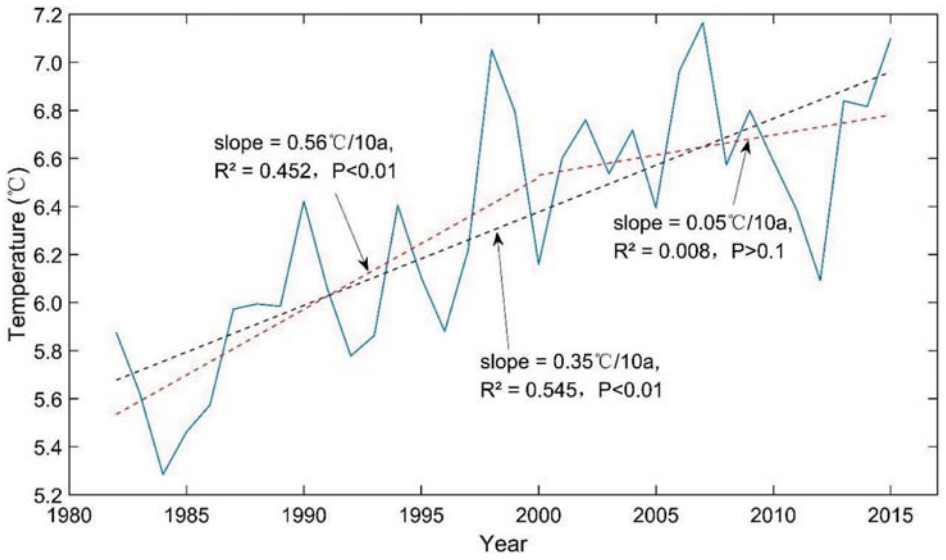


**Figure A1.** Trends in the annual average temperature in mainland China from 1982 to 2015.

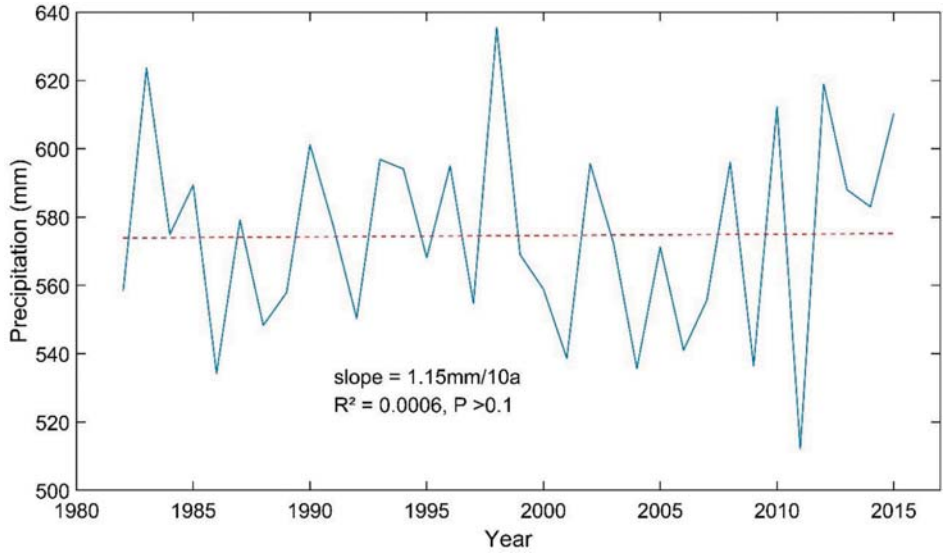


**Figure A2.** Trends in the annual total precipitation in mainland China from 1982 to 2015.

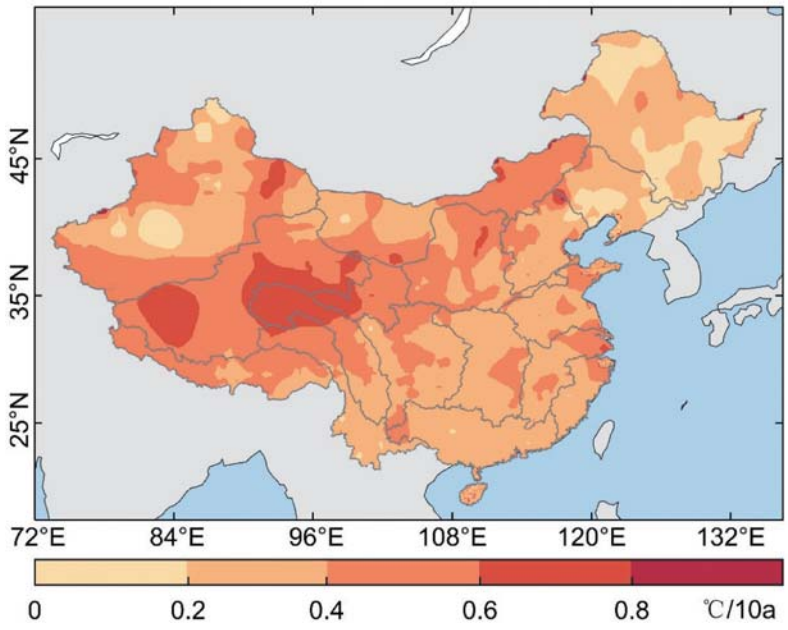


**Figure A3.** Spatial distribution of the slope in the annual average temperature from 1982 to 2015 in mainland China.

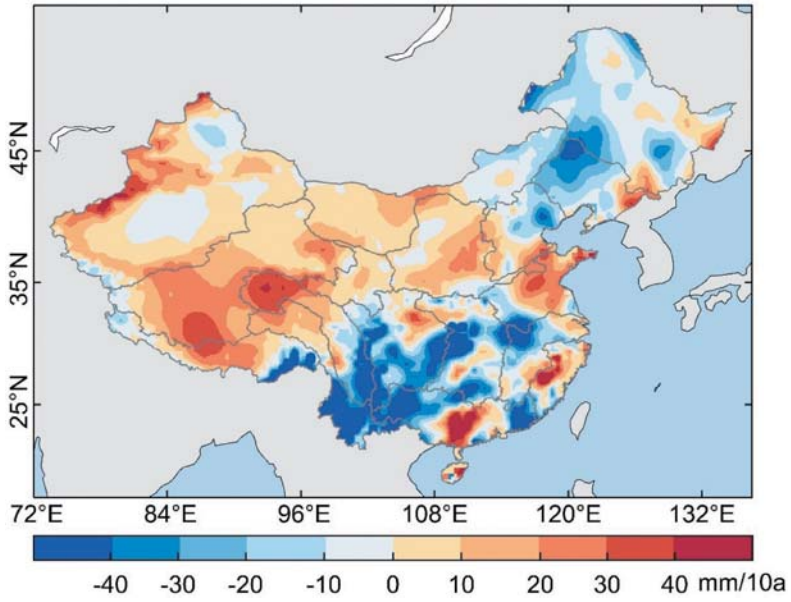


**Figure A4.** Spatial distribution of the slope in the annual total precipitation from 1982 to 2015 in mainland China.